NSG-1425

From: [redacted]
Dept. of Electrical Engineering
College of Engineering
University of Florida
Gainesville, Florida 32611

(NASA-CR-157475) STUDY OF ELECTRONIC PROPERTIES IN PROTON- AND ELECTRON-IRRADIATED GaAlAs AND GaAs SOLAR CELL MATERIALS Final Report, 1 Sep. 1977 - 31 Aug. 1978 (Florida Univ.) 69 p HC A04/MF G3/44

N78-29568

Unclas 27234

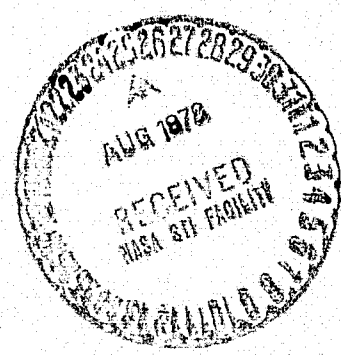

FINAL REPORT

(Covering period: September 1, 1977 - August 31, 1978)

STUDY OF ELECTRONIC PROPERTIES IN PROTON- AND ELECTRON-IRRADIATED GaA&As and GaAs SOLAR CELL MATERIALS

By

Sheng S. Li
Electrical Engineering Department
University of Florida
Gainesville, Florida 32611

NASA Grant No. NSG-1425

This work was performed for the National Aeronautical and Space Administration
Langley Research Center,
Hampton, Virginia 23365

ABSTRACT

This report presents technical findings in one-MeV proton irradiated n-type GaAs during the first year of research supported by NASA grant No. NSG-1425 and University of Florida EIES special project. Diagnostical measurement techniques such as dark I-V, C-V, the TSCAP, and the DLTS methods are employed to study defect properties in the proton-irradiated n-GaAs materials. Defect energy levels, thermal emission rates, and capture cross sections of electrons as well as trap densities are deduced from these measurements, and the results are presented in this report. Correlations between the measured defect parameters and the dark I-V characteristics of the n-GaAs Schottky barrier diodes are also discussed. Defect energy levels (i.e., electron traps) determined in this work are also compared with the published data in order to identify their physical origins.

TABLE OF CONTENTS

I. INTRODUCTION

The goal of this research project is to conduct a detailed study of the electronic properties of defects introduced by high energy electron- or proton-irradiation in GaAs and GaAlAs solar cell materials. It is well known that when semiconductor materials are irradiated by high energy electrons or protons considerable damage (e.g., creation of vacancies, interstitials, vacancy-impurity complex, defect clusters, etc.) results. In fact, electron- or proton-irradiation on semiconductors can usually produce defect centers which may act as recombination or trapping centers for minority carriers and as such lowering the minority carrier lifetimes or diffusion lengths in the material. When these semiconductors are used for solar cell fabrication, the radiation damage would result in degradation of solar cell performance and lowering the conversion efficiency.

In this report we present the initial results of our study of the defect properties in both the unirradiated and one-MeV proton irradiated n-GaAs single crystal specimen.

Experimental tools employed in this study include the I-V and C-V measurements, the deep level transient spectroscopy (DLTS) and the thermally stimulated capacitance (TSCAP) measurements on Schottky barrier diodes fabricated from the undoped n-type GaAs materials. From these measurements we determined the energy levels and the densities of defect centers, the temperature and electric field dependence of electron emission and capture rates associated with each defect level in both the unirradiated- and one-MeV proton-irradiated n-GaAs samples. Dark I-V and C-V measurements were performed on these Schottky barrier diodes to study the effect of proton fluence on the generation-recombination current and the majority carrier removal rates in n-type GaAs materials. Correlations

were obtained among the measured defect parameters and the dark I-V characteristics and minority carrier diffusion lengths in these n-GaAs Schottky diodes.

Our research efforts during this reporting period have been focused mainly on the experimental set-ups for the DLTS and TSCAP measurements, fabrication of ohmic and Schottky contacts on n-type GaAs samples, and the determination of defect parameters in both the unirradiated- and one-MeV proton irradiated n-GaAs samples by using DLTS and TSCAP methods. The results of this effort will be discussed in detail in this technical report.

II. EXPERIMENTAL DETAILS

In this section, we present several experimental tasks that have been accomplished during this reporting period.

2.1 Modification of metal evaporation system:

The evaporation chamber for making ohmic and Schottky contacts on n-type GaAs substrate was modified in our laboratory. Two tungsten basket evaporation shields were installed in our Kenney evaporation system.

The new arrangement allows us to consecutively deposit different metals on GaAs substrate without opening the bell jar in the system. This permits clean evaporation and reduces the risks of contamination during successive metal depositions.

The evaporation shield unit consists of two side arms which fit filament posts. Each arm supports a chrome-plated disc. An annealed Pyrex tube slides over the discs and is held firmly in place by a coil spring.

Controlled evaporation is done through a carefully dimensioned slot (1 cm wide) in the Pyrex tube (3 cm in diameter and 8 cm long) which corresponds accurately with a hole in the metal shield. Both Pyrex tube and metal shield can be rotated to allow coating or shadowing from any desired angle.

This modified evaporation system has been used routinely for the fabrication of ohmic and Schottky barrier contacts on GaAs substrates. Good ohmic and Schottky barrier contacts on n-GaAs have been obtained from this system.

2.2 Preparation of Ohmic and Schottky contacts on n-type GaAs

The undoped n-type GaAs with electron density of around 2×10^{16} cm^{-3} was used for the present study. The wafer is 16 mils (0.04 cm) thick with one side chemically polished and the other side mechanically polished.

Prior to making ohmic and Schottky contacts, the wafer was cleaned thoroughly using procedures reported by Stirn and Yeh [1]. This includes the use of degreasing solution (i.e., NH_4OH : H_2O_2 : H_2O - 10:1:1 in volume) and sulfuric-peroxide etching solution (H_2SO_4 : H_2O_2 : H_2O - 8:1:1 in volume). The ohmic contact was made on the mechanically polished side, using the following procedures: The GaAs wafer was first placed on a ceramic plate holder inside the evaporation chamber, and then heated to 210°C to remove the residual organic contaminants on the surface. The wafer was allowed to cool down to room temperature, and the Au-Ge (88-12%) alloy which was placed in a tungsten basket, was then evaporated onto the GaAs substrate. Following Au-Ge evaporation, the wafer was heated to 360-370°C and then cooled down inside the evaporation chamber. This final heating was accomplished at a temperature slightly higher

than the melting point of Au-Ge eutectic and thus enables the alloying of Au-Ge onto GaAs substrate to form a good ohmic contact. An additional step may be taken by evaporating a thin nickel film on top of an Au-Ge layer to improve bonding [2].

Schottky barrier contact was made on the chemically polished side of the GaAs substrate. A metal mask with 30 mil (~0.075 cm) holes located 60 mil apart was used to deposit the aluminum dot onto the GaAs substrate to form Schottky contact. The reason for choosing aluminum over gold for Schottky contact was that aluminum has excellent adhesion to GaAs and is easier for ultrasonic wire bonding and convenient for proton irradiation.

The fabricated GaAs Schottky diode has an active area of 4.56×10^{-3} cm^2. To facilitate proton-irradiation and defect measurements, each diode was mounted on a gold plated sapphire pedestal. Conductive silver epoxy was used to bond the ohmic contact of the diode onto the sapphire plate. Gold wire was ultrasonically bonded to the aluminum dot for the Schottky contact. The diode-sapphire chip, mounted on TO-5 header was then used for proton irradiation and other measurements.

2.3 Proton irradiation for n-GaAs Schottky diodes

A specially designed sample holder for proton-irradiation was constructed in our laboratory. The holder is a water-cooled copper block which can hold up five diodes for room temperature irradiation. The sample holder was connected to a stainless steel coaxial waterline shaft which mates through a vacuum interlock to the irradiation chamber. For proton-irradiation, the TO-5 header in which the GaAs diode was housed, was covered with a metal cap which has a hole slightly larger than the GaAs diode. This cap acts as a Faraday cup, which can suppress secondary emission from the GaAs diode, by applying a negative voltage of 70 to 90 V

to the metal cap. The schematic diagram of the sample holder used in our proton-irradiation is shown in Fig. 1.

The proton source was obtained from a van de Graff linear accelerator located in the Physics Department of the University of Florida. This machine can produce proton beams with energies ranging from 0.5 to 3 MeV. One-MeV proton energy was used in the present study. Four GaAs Schottky barrier diodes were subsequently irradiated by one-MeV proton with fluence given respectively by 5.8×10^{12}, 4.5×10^{13}, 4.4×10^{14}, and 4.1×10^{15} cm^{-2}, as measured by a charge integrator. The projected range of penetration depth for different ions as a function of energy in GaAs, Si, and Zr is shown in Fig. 2. For one-MeV proton (H), the projected range is around 9~10 μm in GaAs.

2.4 Measurement techniques for defect characterization

In the present work we have employed the thermally stimulated capacitance (TSCAP) [3], and the deep-level transient spectroscopy (DLTS) measurement techniques for defect characterization in both unirradiated and proton-irradiated n-type GaAs specimen. Since a Schottky barrier structure was used, only the majority carrier traps (i.e., electron traps) were investigated in the present study. Information on defect energy levels and defect densities, as well as, electron emission and capture rates can be readily obtained from these measurements.

The experimental set-ups for the TSCAP and DLTS measurements are well documented in the literature [3-4]. The DLTS measurement technique is by far the most sensitive and effective method for defect inventory and characterization [4]. This method is particularly suitable for studying the deep level defects with fast emission rates. However, the TSCAP experimental set up which is much simpler than the DLTS method,

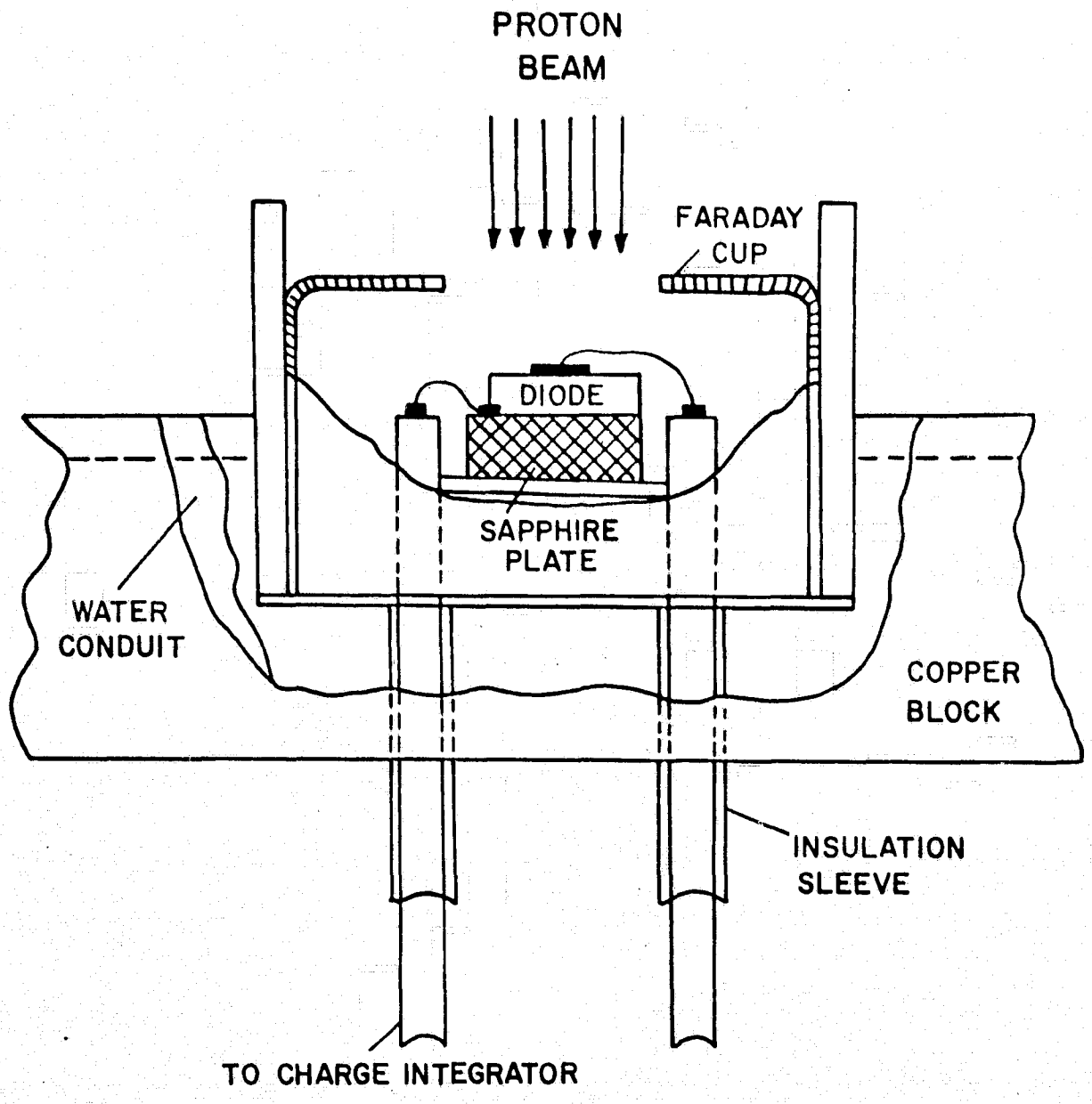

Fig. 1 Sample holder for proton irradiation.

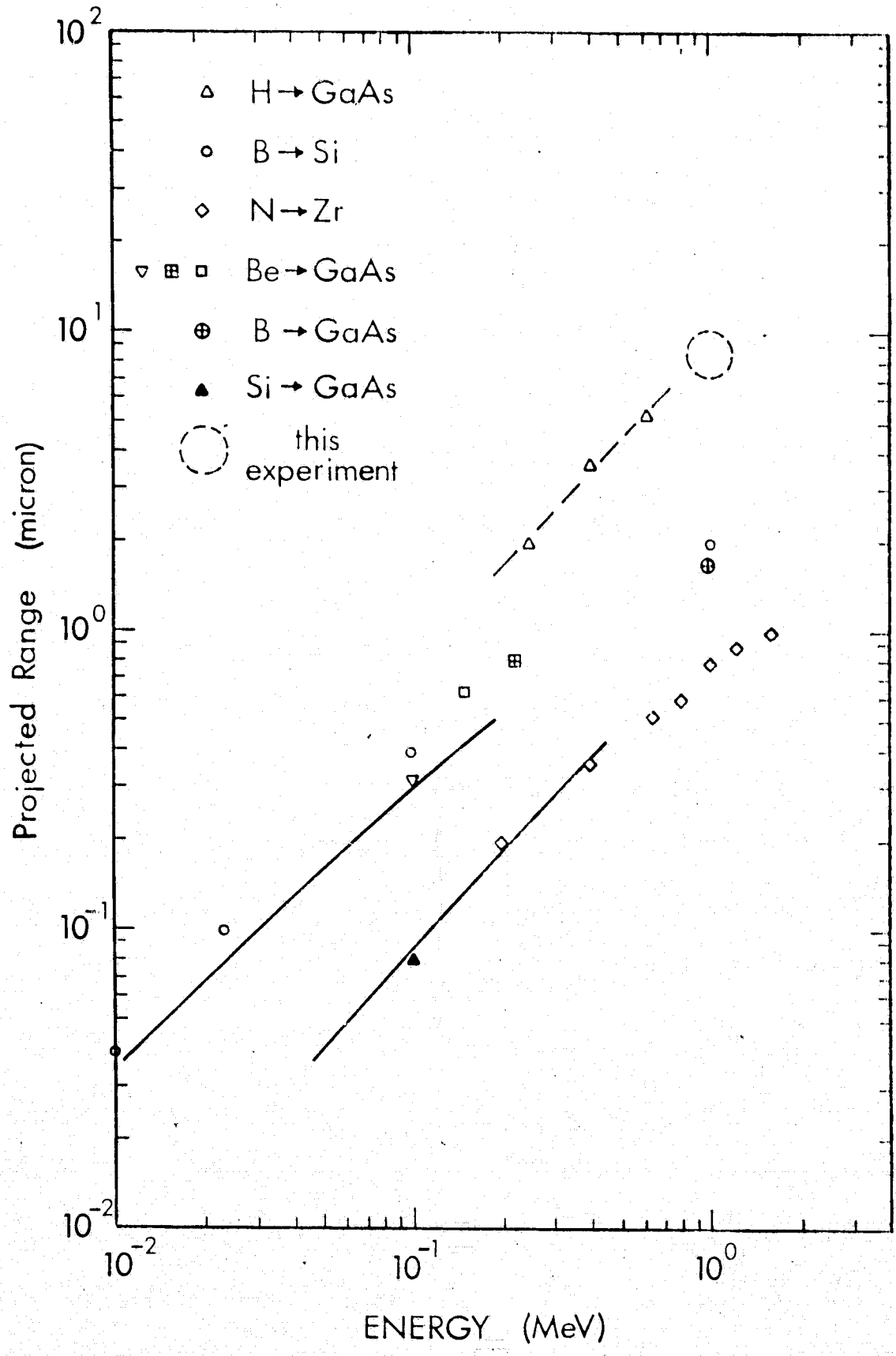

Fig. 2 The projected Range of Penetration Depth versus Energy of Different Ions in GaAs, Si , and Zr. The proton ion (H) projected range is about 10 μm at 1 MEV in GaAs.

can also provide a quick scan of the deep level impurities and defects in the semiconductor material.

In brief, the TSCAP experimental set-up consists of a capacitance meter, an X-Y recorder, a power supply, and a liquid nitrogen dewar system for temperature control. The experimental set-up for the TSCAP measurements is relatively simple and inexpensive.

As for the DLTS experimental set-up, the system is considerably more complex than that of the TSCAP method. As shown in Fig. 3, the system consists of a pulse generator, an RF signal generator, an RF capacitance bridge, a wide band preamplifier, a mixer and the delay lines, gate integrators and a box averager, an oscilloscope and an X-Y recorder, and a liquid nitrogen cryogenic temperature controller. This system is operated at 20 MHz and hence is more sensitive than the TSCAP system which is operating at 1 MHz.

In addition to the TSCAP and the DLTS measurements, the I-V and C-V measurements are also employed to study the generation-recombination (g-r) current in the space charge region and the majority carrier density in the proton-irradiated and the unirradiated GaAs Schottky diodes. These measurements can also provide additional information concerning the recombination and trapping mechanisms in the GaAs materials.

Experimental set-ups for the surface photovoltage (SPV), photoconductivity (PC) and photomagnetoelectric (PME) measurements have also been undertaken. These measurements will permit the determination of the minority carrier diffusion lengths and lifetimes in GaAs. This will enable us to correlate the measured diffusion length with defect parameters determined by the DLTS method.

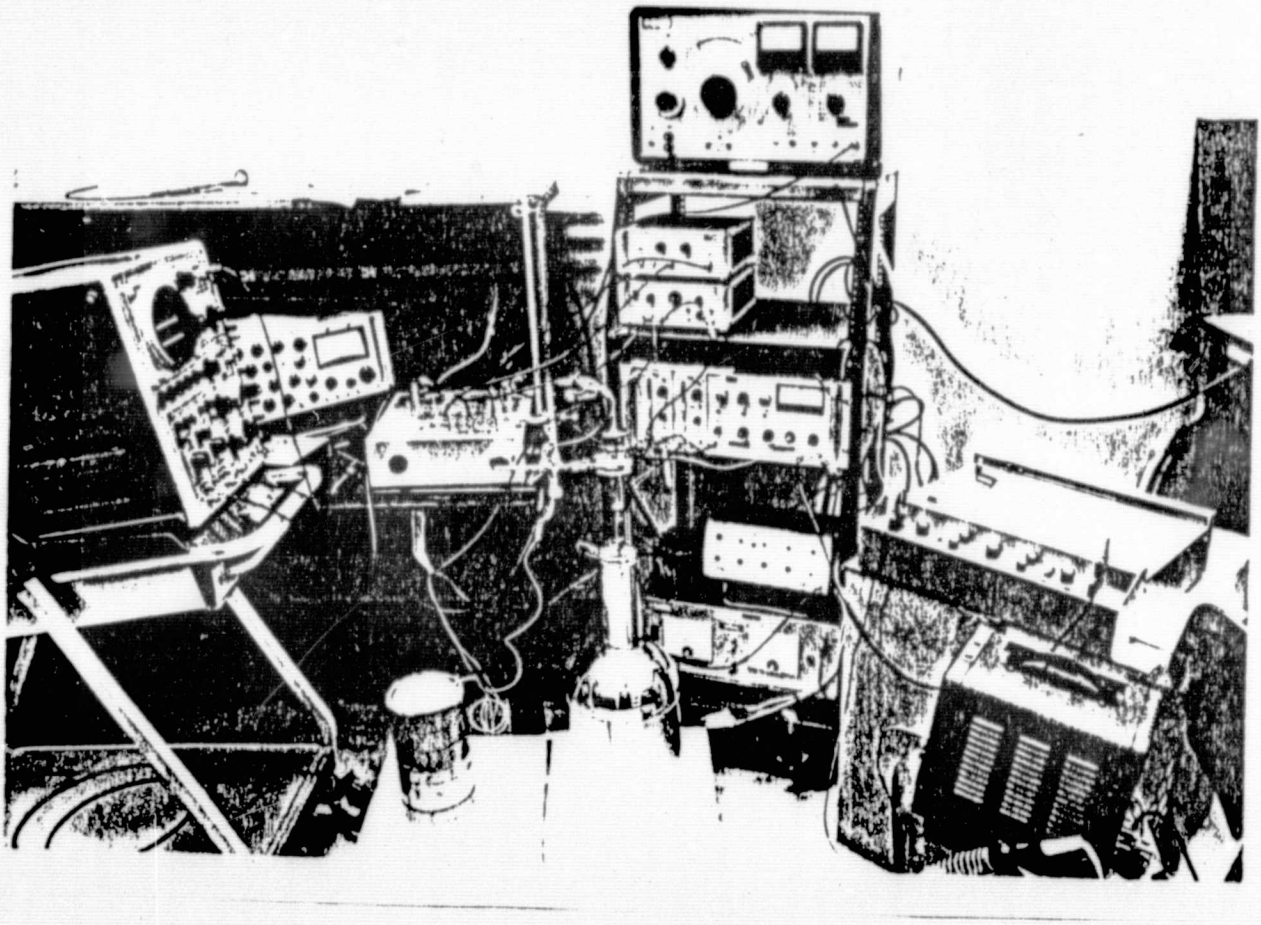

Fig. 3 Experimental set-up for DLTS measurements.

III. RESULTS AND DISCUSSIONS

In this section we present the experimental results for both unirradiated and one-MeV proton irradiated n-GaAs Schottky diodes. Important physical parameters of the defects such as energy levels, defect density, electron thermal emission and capture rates, as well as nature of each defect level, are determined for these samples. Furthermore, good correlation between the measured defect parameters and the I-V characteristics of the irradiated diodes are also obtained in the present study.

3.1 Interpretation of the I-V data

Current-voltage (I-V) and capacitance-voltage (C-V) measurements were performed on all GaAs Schottky barrier diodes before and after proton-irradiation. From these measurements, the barrier height, the substrate dopant density, and the ohmic contact properties are evaluated.

A typical plot of the I-V curves as a function of temperature under forward bias conditions for an unirradiated GaAs Schottky diode (i.e., SD-231) is shown in Fig. 4. Based on thermionic emission theory, the I-V characteristics curve for a Schottky diode can be described by [7]:

$$I = I_o\left[\exp\left(\frac{qV}{nk_oT}\right) - 1\right] \tag{1}$$

where

$$I_o = AA^*T^2\exp\left(-\frac{q\phi_{Bn}}{k_oT}\right) \tag{2}$$

is the dark saturation current and ϕ_{Bn} is the barrier height; n is the diode ideality factor.

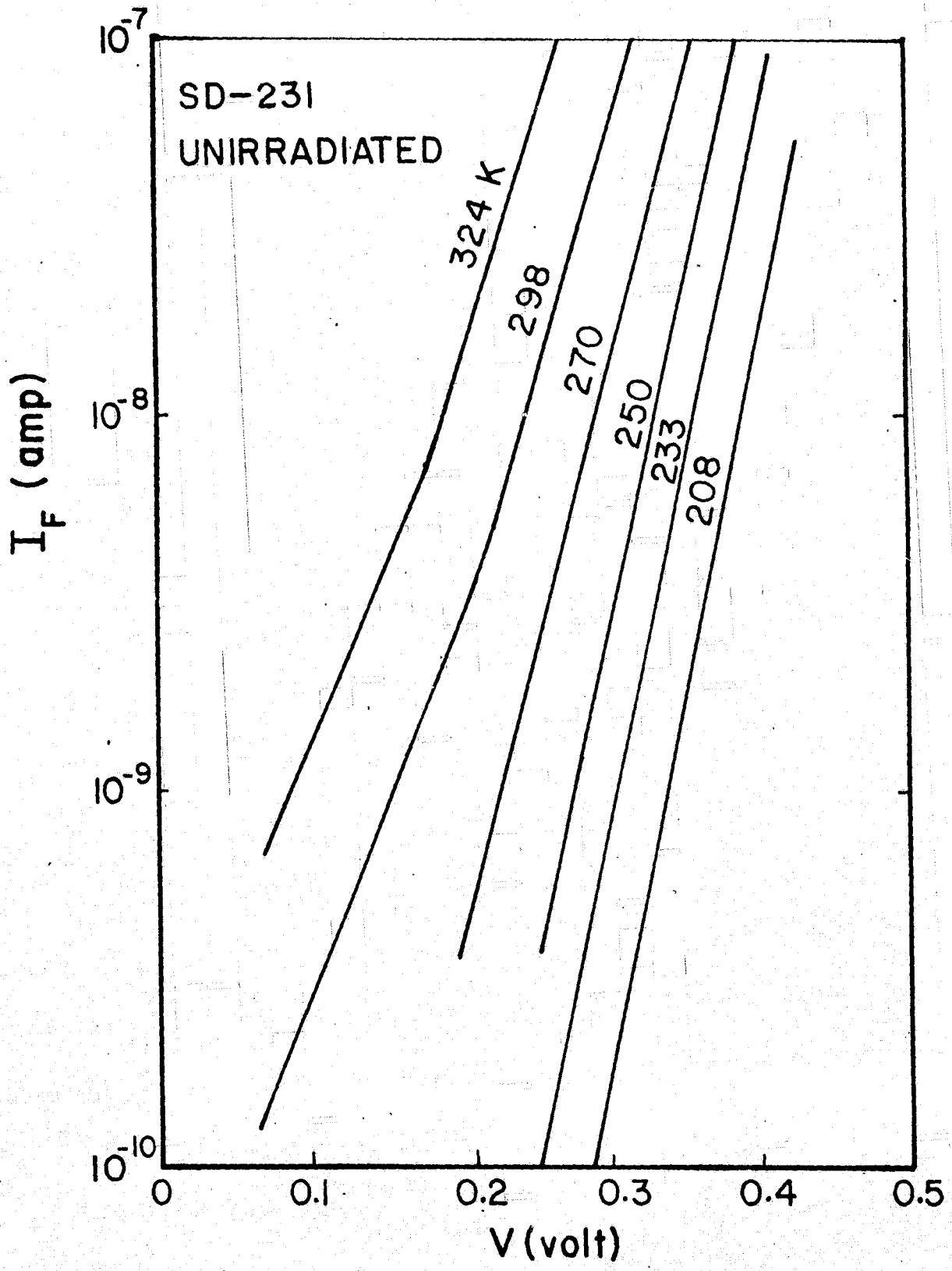

Fig. 4 Forward I-V characteristic curves as a function of temperature for an un-irradiated Al- n GaAs Schottky barrier diode

Both ϕ_{Bn} and n can be deduced from Fig. 4, using eqs. (1) and (2). The barrier height for these diodes is found to be around 0.95 eV, and the diode ideality factor, n, at higher bias voltages ($\geq$ 0.4V) varies between 1.2 to 1.5.

To study the effect of proton irradiation on the generation-recombination (g-r) current in n-GaAs Schottky diodes, we measured the reverse and forward I-V characteristic curves for both the unirradiated and proton-irradiated GaAs Schottky diodes at 300K. The results are shown in Fig. 5 and Fig. 6 . Diodes SD-234 and SD-231 are unirradiated, and diodes SD-233, 232, 143, 142 are proton-irradiated with increasing fluence. The results clearly show that the reverse saturation current of the diode is higher for the proton irradiated samples than for the unirradiated diodes. To explain this, we note that the reverse saturation current for a Schottky diode can be described by eq. (2) (i.e., the thermionic emission current) only if the (g-r) current is negligible. However, when the (g-r) current becomes important as a result of the increase in the density of (g-r) defect centers induced by proton irradiation, it is necessary to include the (g-r) current component in eq. (1) for the Schottky diode. This is clearly shown in Fig. 5 where the dash line is for the saturation current, I_o, calculated from eq. (2) for GaAs. The (g-r) current in the space charge region of the diode can be described by [8]:

$$I_{gr} = qAWN_T e_p^t \qquad (3)$$

where N_T is the density of (g-r) defect centers

AW product is the volume of space charge region

e_p^t is the hole emission rate.

In eq. (3) we have assumed that the electron emission rate is much greater than the hole emission rates. The (g-r) current is directly proportional to the depletion layer width, W, which in turn varies as the square root of the reverse bias voltage for a Schottky diode. Thus, the voltage dependence of the reverse current gives a direct means to determine the (g-r) current component. The results shown in Fig. 5 indicate that except for diode SD-234 (i.e., the unirradiated diode), all the irradiated diodes have their reverse saturation current dominated by the (g-r) current component in the low reverse bias voltage region. The results further show that the proton-irradiated diodes have a much larger reverse saturation current than those of the unirradiated diodes. Fig. 7 shows the reverse saturation current as a function of the proton fluence for four proton-irradiated n-GaAs Schottky diodes at $V_R = -5$ volts. The results illustrate that for $\phi_o > 10^{13}$ cm^{-2} the reverse saturation current increases with increasing proton fluence. The fact that diode SD-233 has the highest reverse saturation current among all the irradiated diodes is consistent with the results observed in the forward I-V characteristics and the TSCAP and DLTS measurements to be discussed later.

The role of proton irradiation induced defects which may serve as generation-recombination (g-r) centers in the space charge region of the Schottky barrier or p-n junction diode can also be studied through the analysis of the forward I-V characteristics curves. Fig. 6 shows the forward I-V characteristic curves for one unirradiated and four proton-irradiated diodes. The Schottky diode equation under forward bias condition, taking into account the recombination current in the space charge region, can be expressed by:

$$I_F = I_{n1} \exp\left(\frac{qV}{n_1 kT}\right) + I_{n2} \exp\left(\frac{qV}{n_2 kT}\right) \quad (4)$$

where

$$I_{n1} = \frac{qWn_i A}{2\tau_i} , \quad (5)$$

I_{n1} is the recombination current component in the space charge region; n_1 has a value varying between 2 and 4 depending on the number of recombination centers presented in the diode.

The second term in eq. (4) is identical to eq. (1), and I_{n2} is given by eq. (2). Also, n_2 in eq. (4) is the diode ideality factor which is usually greater than one for GaAs Schottky barrier diode. From the I-V curves displayed in Fig.6, it is shown that at low forward bias voltage ($V_F \leq 0.2V$), the I-V characteristics are dominated by the recombination current in the space charge region of the diode; the value of n_2 varies between 2 and 4 indicating multi-level recombination centers contributed to the total recombination current [8]. In addition, the result further shows that the recombination current also increases with increasing proton fluence in the diodes (with the exception of diode SD-233, which again has the largest recombination current among all the irradiated diodes).

From the foregoing analyses, we conclude that one-MeV proton irradiation in n-GaAs introduces additional (g-r) defect centers which in turn produces higher reverse saturation current and forward recombination current. This has a detrimental effect on the open circuit voltage of a solar cell [9].

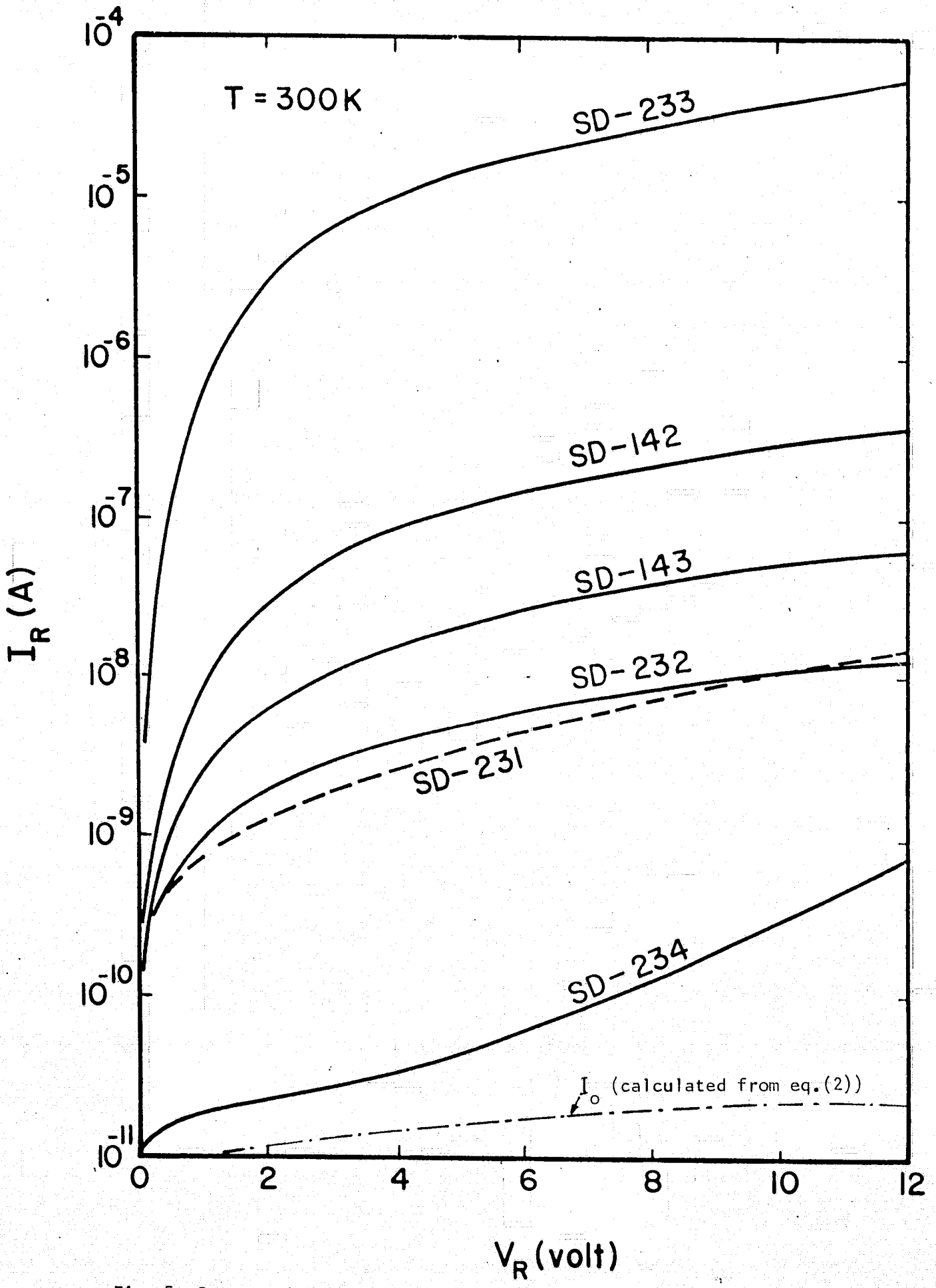

Fig. 5 Reverse I-V characteristic curves for un-irradiated and one- MeV proton irradiated n-type GaAs Schottky diodes

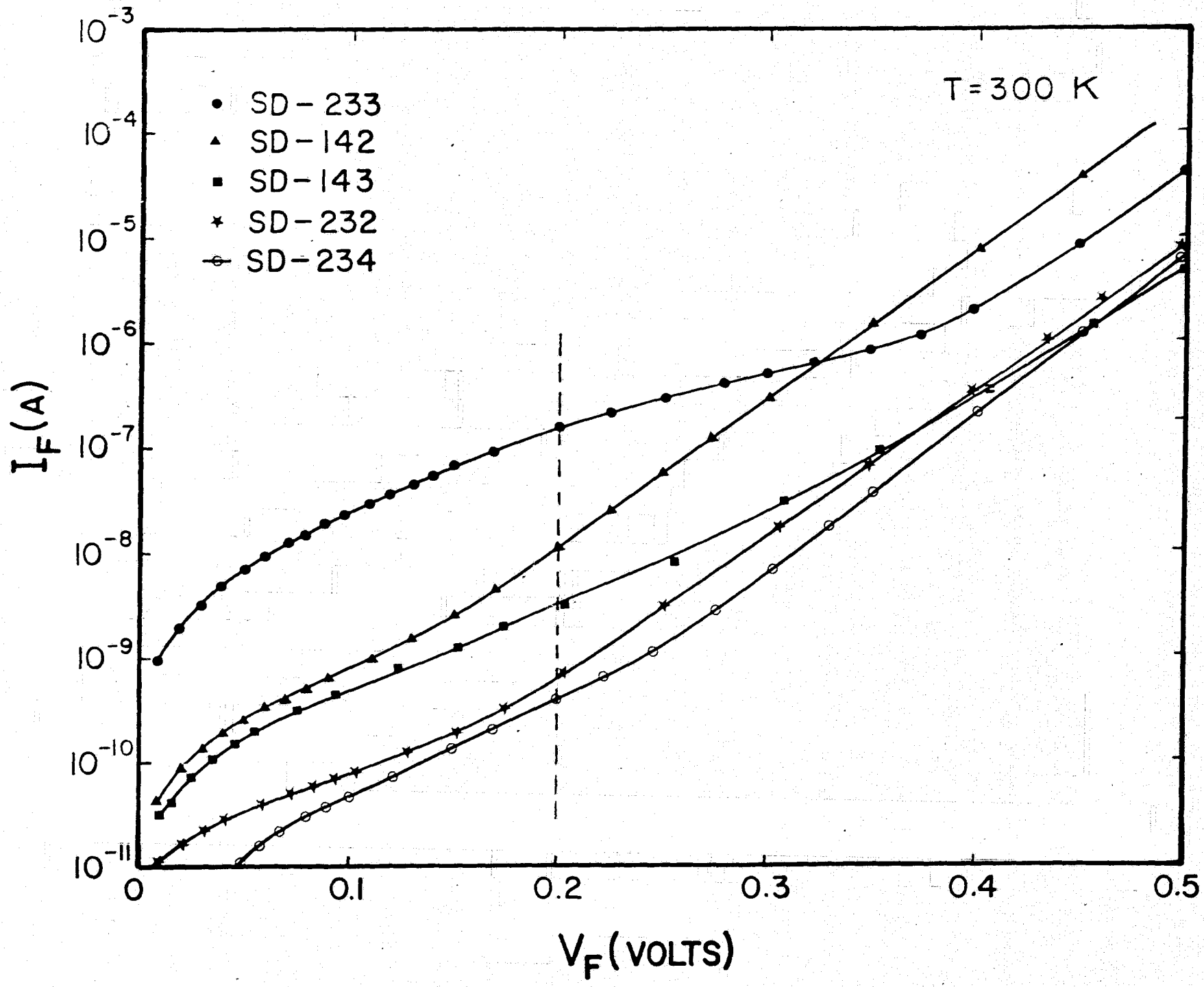

Fig. 6 Forward I - V Characteristic curves for five n-GaAs Schottky Barrier Diodes

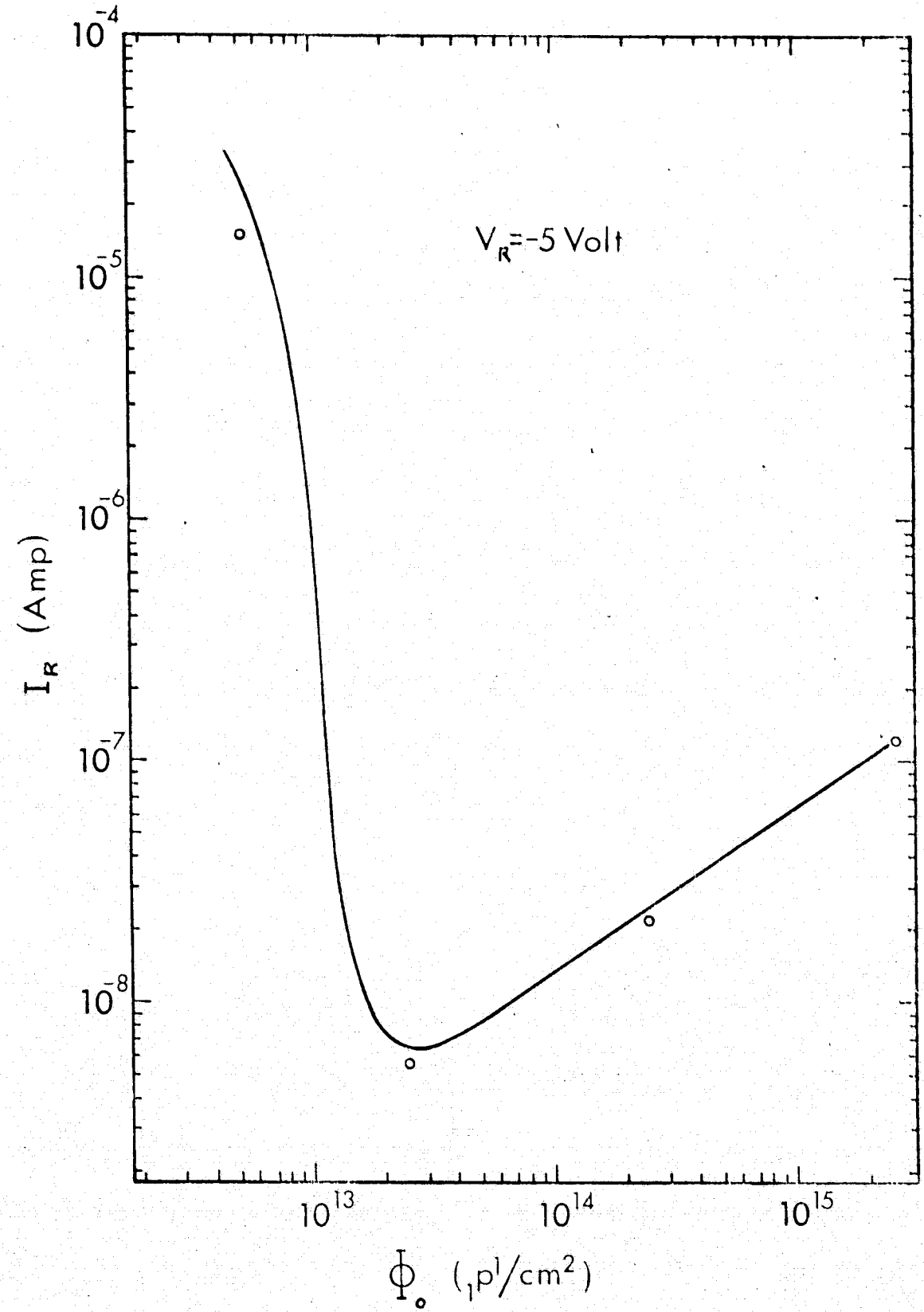

Fig. 7 Reverse saturation current versus proton fluence for four proton-irradiated n-GaAs Schottky diodes

3.2 Interpretation of the C-V data

We next discuss the results of our steady state capacitance-voltage (C-V) measurements on these diodes. From the C-V measurements, the majority carrier density in n-GaAs substrate is determined. The C-V plots under reverse bias conditions for both unirradiated and proton-irradiated diodes are displayed in Fig. 8 and Fig. 9, respectively. The decrease in capacitance with increasing proton fluence is clearly demonstrated in these figures. This is a direct result of the reduction in majority carrier density with increasing proton fluence in the n-GaAs substrates.

The electron density in n-GaAs substrate can be determined from the C^{-2} versus V plot using the following expression:

$$n_o(x) = \left(\frac{C^3}{q\varepsilon_o\varepsilon_s A^2}\right) \frac{dV}{dC} \qquad (6)$$

Fig 10 shows the calculated electron density as a function of the reverse bias voltage for the pre- and post-irradiated n-GaAs Schottky diodes. A reduction in electron concentration by more than one order of magnitude was observed in this figure, as a result of the proton irradiation in these diodes. As shown in Fig. 2, the penetration depth of one MeV proton in GaAs is around 9μm with a standard deviation of the proton implanted profile of about 2μm width. The reduction of majority carrier density in n-GaAs can be interpreted as directly resulting from the creation of Frankel defects or formation of vacancy-defect complexs by the proton bombardment in the GaAs substrate.

Although the analysis of I-V and C-V data discussed above does not provide a quantitative interpretation of the proton-irradiation on

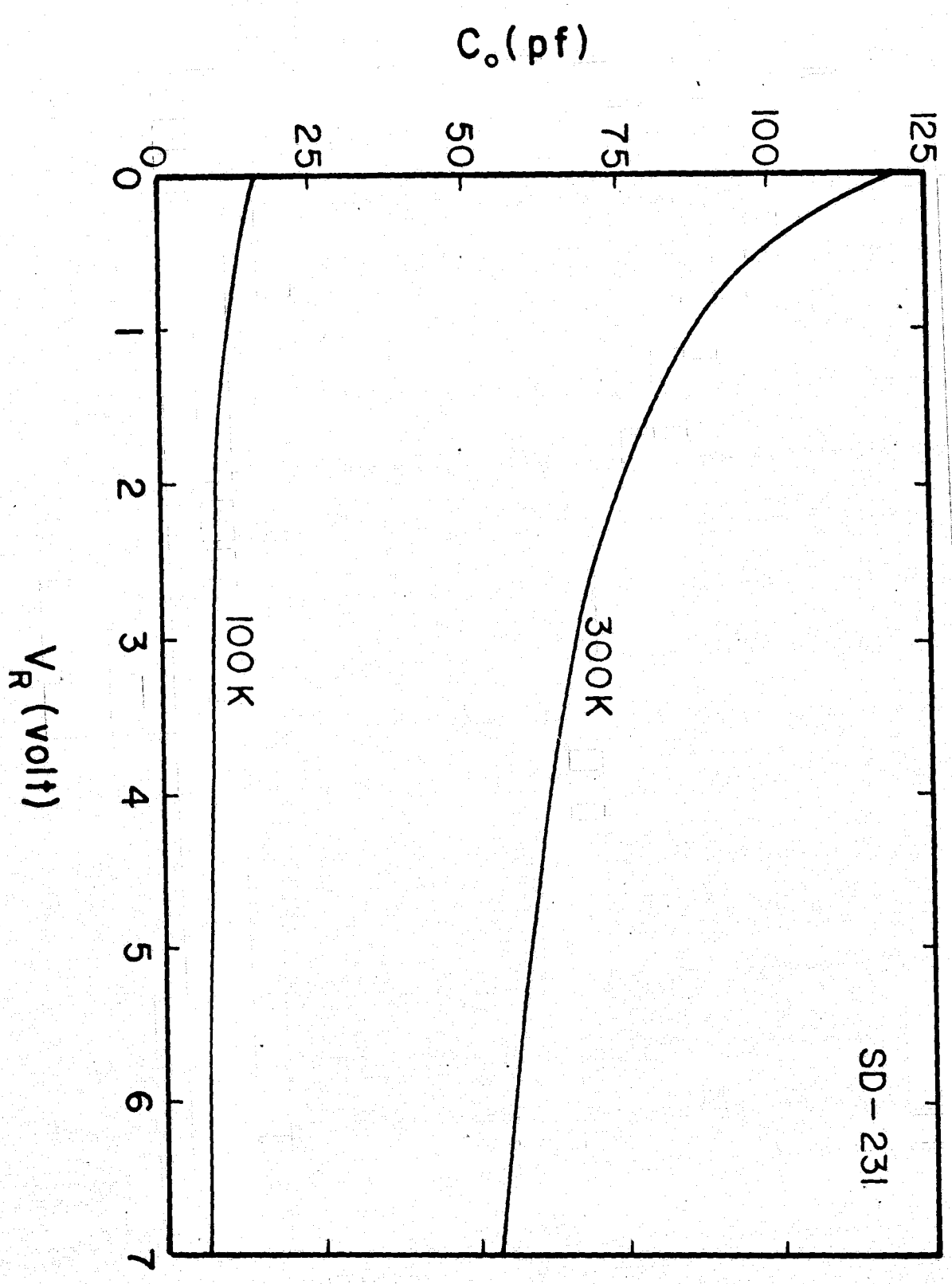

Fig. 8 Capacitance-voltage curve under reverse biased condition for an un-irradiated n-type GaAs sample at T =100,300 K.

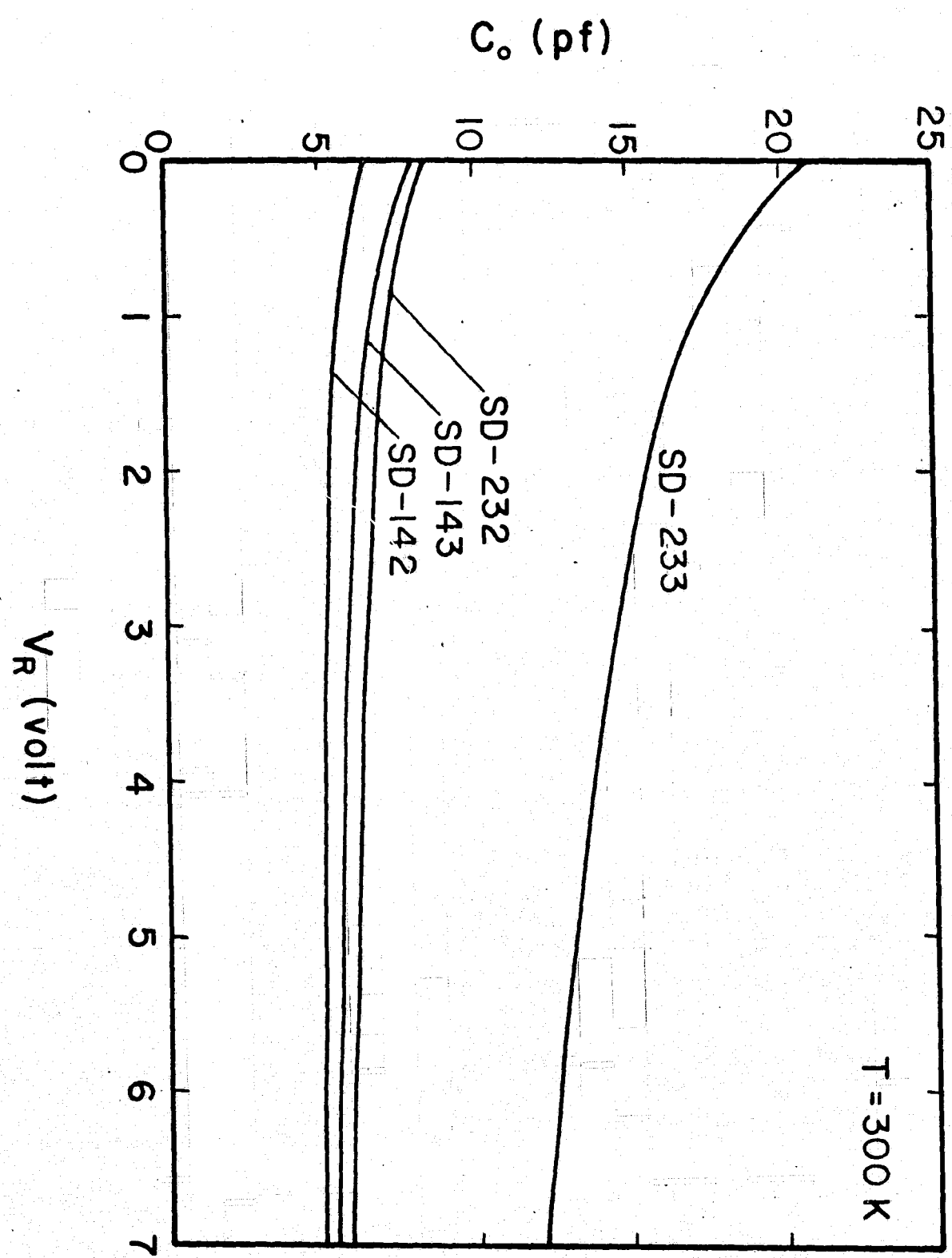

Fig. 9 Capacitance-voltage curve under reverse biased condition for four one-MeV proton irradiated n-type GaAs samples of different proton fluences at T = 300 K.

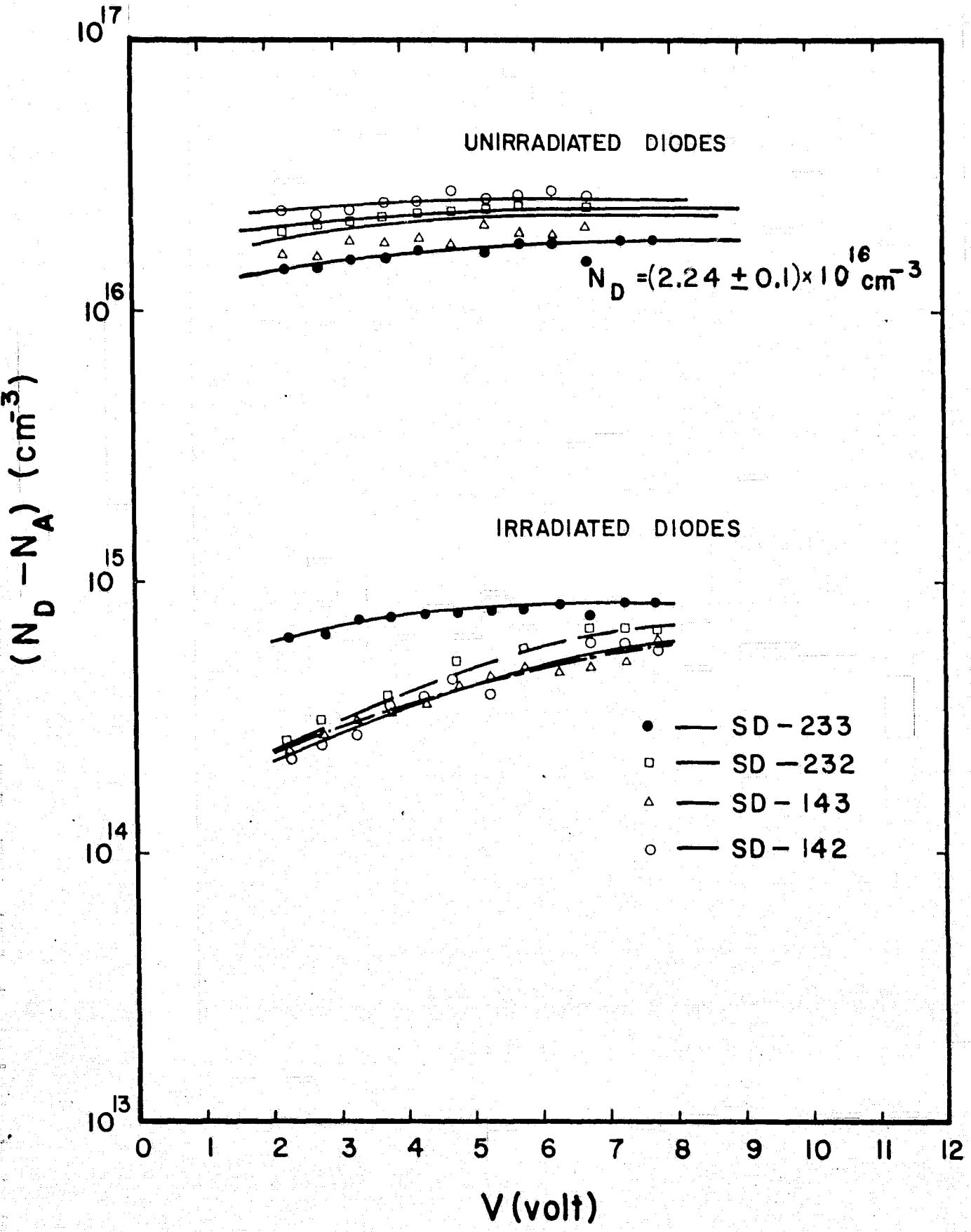

Fig. 10 Majority carrier densities versus reverse biased voltage in the unirradiated and one-MeV proton irradiated n-GaAs Schottky barrier diodes.

defect properties in n-GaAs, it does reveal some important information concerning the radiation damage in the proton-irradiated n-GaAs samples. To obtain quantitative analysis of the defect properties in proton-irradiated GaAs, it is necessary to employ a more sophisticated measurement technique such as TSCAP or DLTS method. We shall discuss these next.

3.3 Results of the TSCAP measurements

As mentioned in Section I, the TSCAP measurements can provide a rapid scan of the deep-level defects which are majority carrier traps (i.e., electron traps) in n-type GaAs samples. The procedure for the TSCAP measurements is depicted briefly as follows: the diode is first cooled to a temperature (e.g., 77K) such that the emission rates are negligible. The diode is zero biased momentarily and then heated at a constant rate. In a characteristic temperature range related to the activation energy of the defect level, the emission rate becomes large enough for all the trapped electrons to be thermally emitted to the conduction band and swept out of the depletion region. This results in an increase in the charge density in the space charge region of the diode and a corresponding capacitance increase. There will be one of these capacitance steps for each activation energy in the upper half of the band gap. The magnitude of each capacitance step can be shown to be related to the defect density producing the capacitance step, and the defect density can be calculated from [8]

$$N_T \simeq \left(\frac{2\Delta C}{C_o}\right)(N_D - N_A) \tag{7}$$

where ΔC is the magnitude of the capacitance step, C_o is the capacitance after electron emission, N_T is the defect density, and N_D is the background impurity density which is determined from C^{-2} vs. V_R via eq. (6).

Equation (7) is valid for $N_T \leq 0.1\ N_D$, and that N_T and N_D are constant across the depletion layer.

The results of the TSCAP measurements on both unirradiated and proton-irradiated GaAs Schottky diodes are shown in Fig. 11 through Fig. 14. Fig 11 shows the TSCAP thermal scan for the unirradiated diode SD-234. The dash line is for the case when a constant reverse bias voltage (i.e., -5V) is applied to the diode during the cooling-heating cycle of the TSCAP scan. The decrease in capacitance with decreasing temperature is due to the freeze out of the majority carriers in the shallow donor levels. The solid line is the result of a typical TSCAP scan. In this case, three distinct capacitance steps were observed in this unirradiated diode which corresponds to three defect energy levels (i.e., electron traps) in the upper half of the band gap. The density of the defects can be calculated from eq. (7) for each capacitance step. The activation energy for each defect level can be determined from the emission rate measurements to be discussed later.

Fig. 12 shows the TSCAP scan for the proton-irradiated diode, SD-233, with $\phi_o = 5.8 \times 10^{12}\ cm^{-2}$. Five main capacitance steps corresponding to five electron traps were observed in this diode for $77 \leq T \leq 400$ K. Fig. 11 and Fig. 12 show the TSCAP scans for two other proton-irradiated diodes, SD-232 and SD-142. The results also show three distinct capacitance steps corresponding to three main electron traps in these samples.

No significant difference in the shape of the capacitance steps in these two diodes when compared with other unirradiated samples exists. The reduction in the total capacitance in the TSCAP scan can be attributed to the decrease in the electron density in these proton-irradiated diodes.

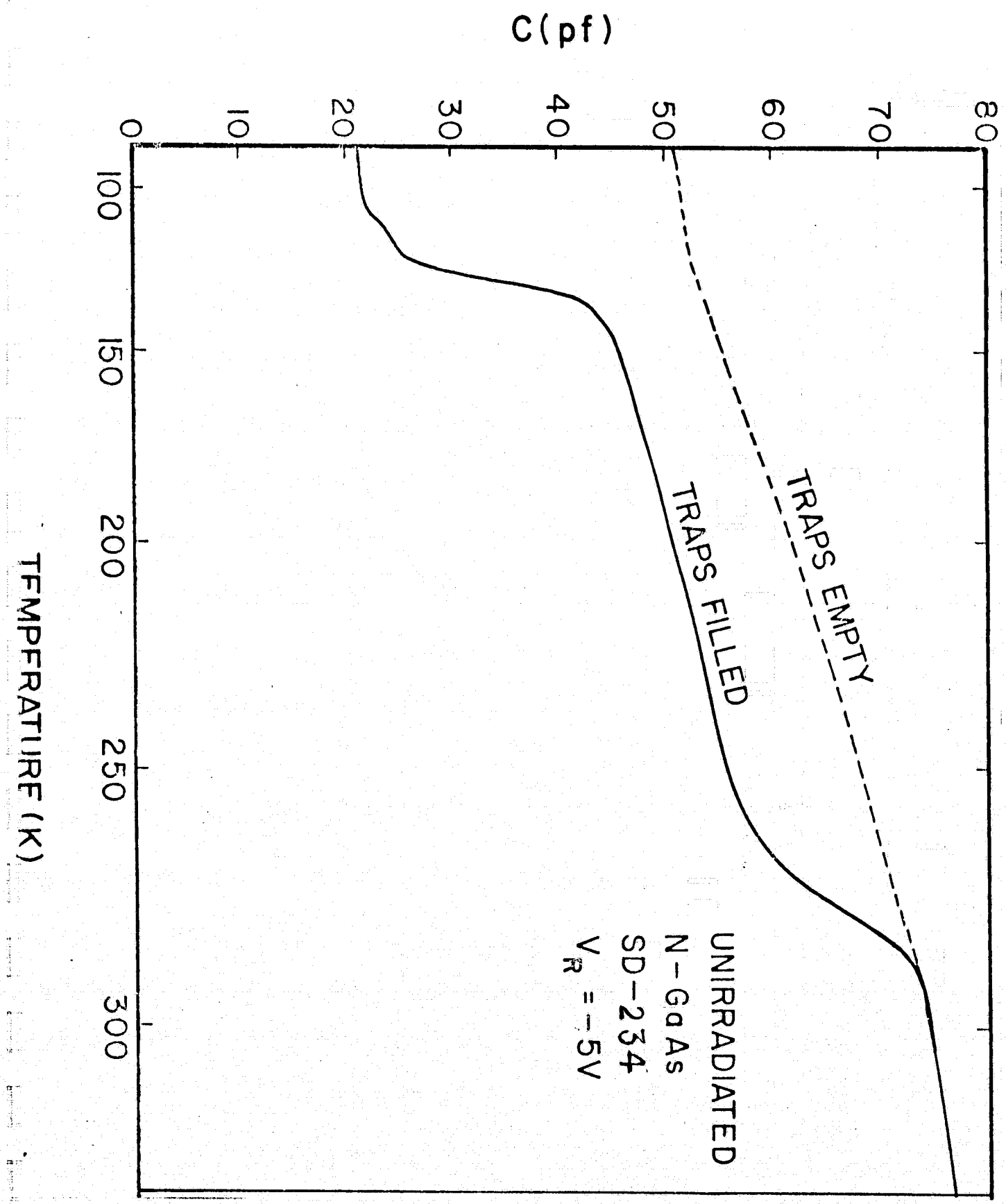

Fig. 11 Thermally stimulated capacitance (TSCAP) response of an un-irradiated Al- n type GaAs Schottky barrier diode. The three capacitance steps represent three electron trap levels.

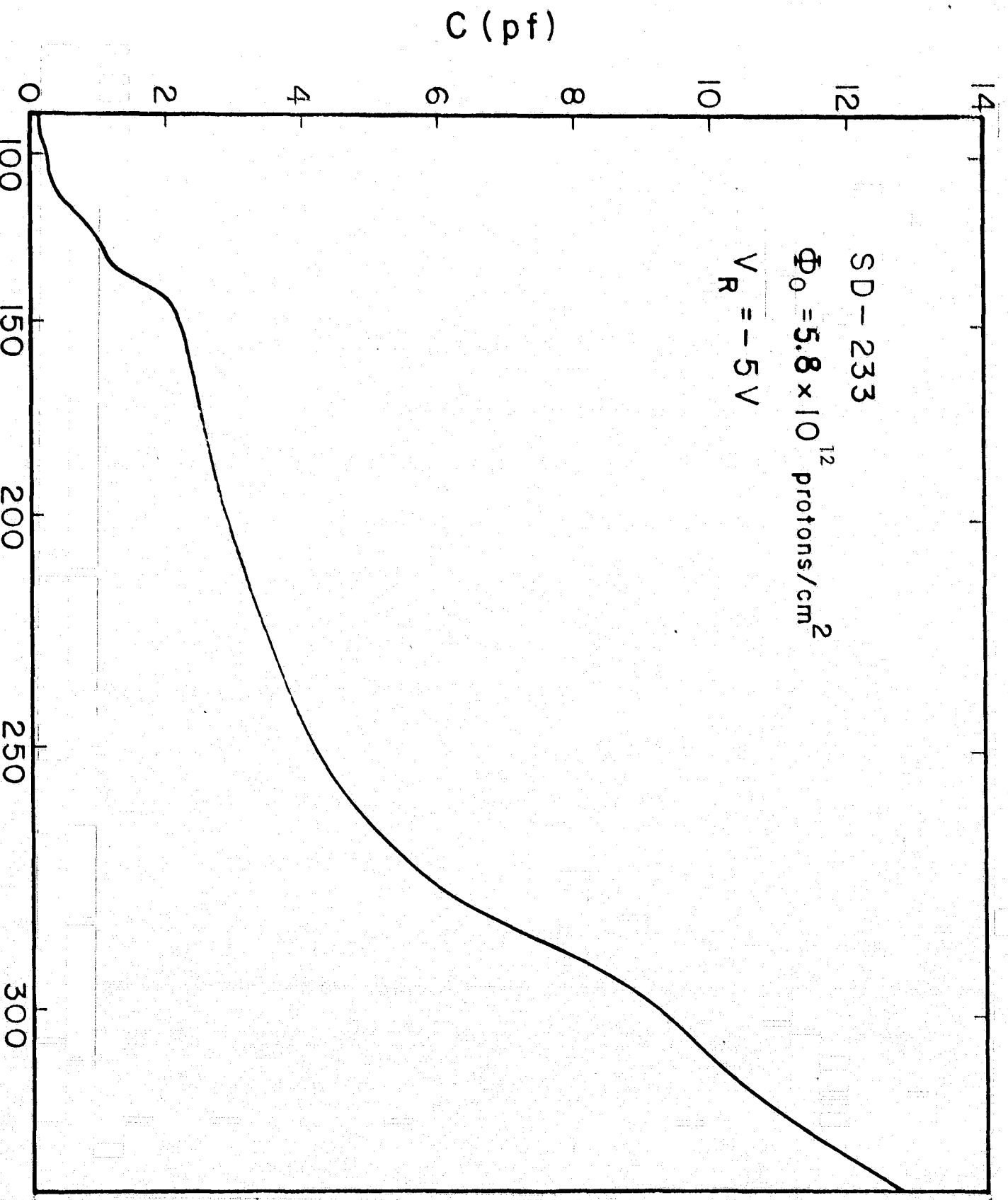

Fig.12 The TSCAP scan of an one- MeV proton irradiated n-GaAs Schottky diode. The five capacitance steps observed in this sample corresponding to five main electron traps.

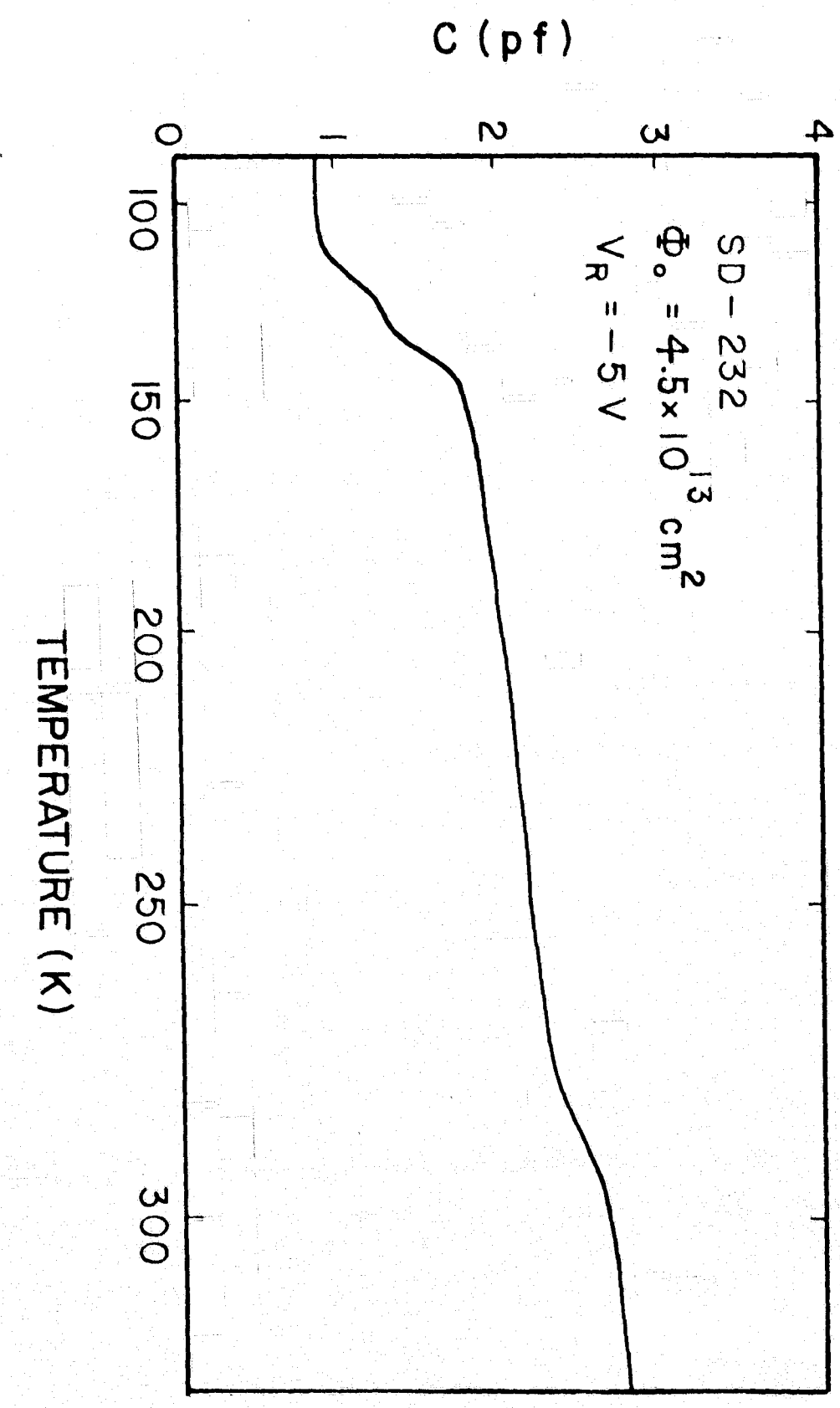

Fig.13 The TSCAP scan of an one-MeV proton irradiated n-type GaAs Schottky barrier diode. Three capacitance steps were observed in this sample.

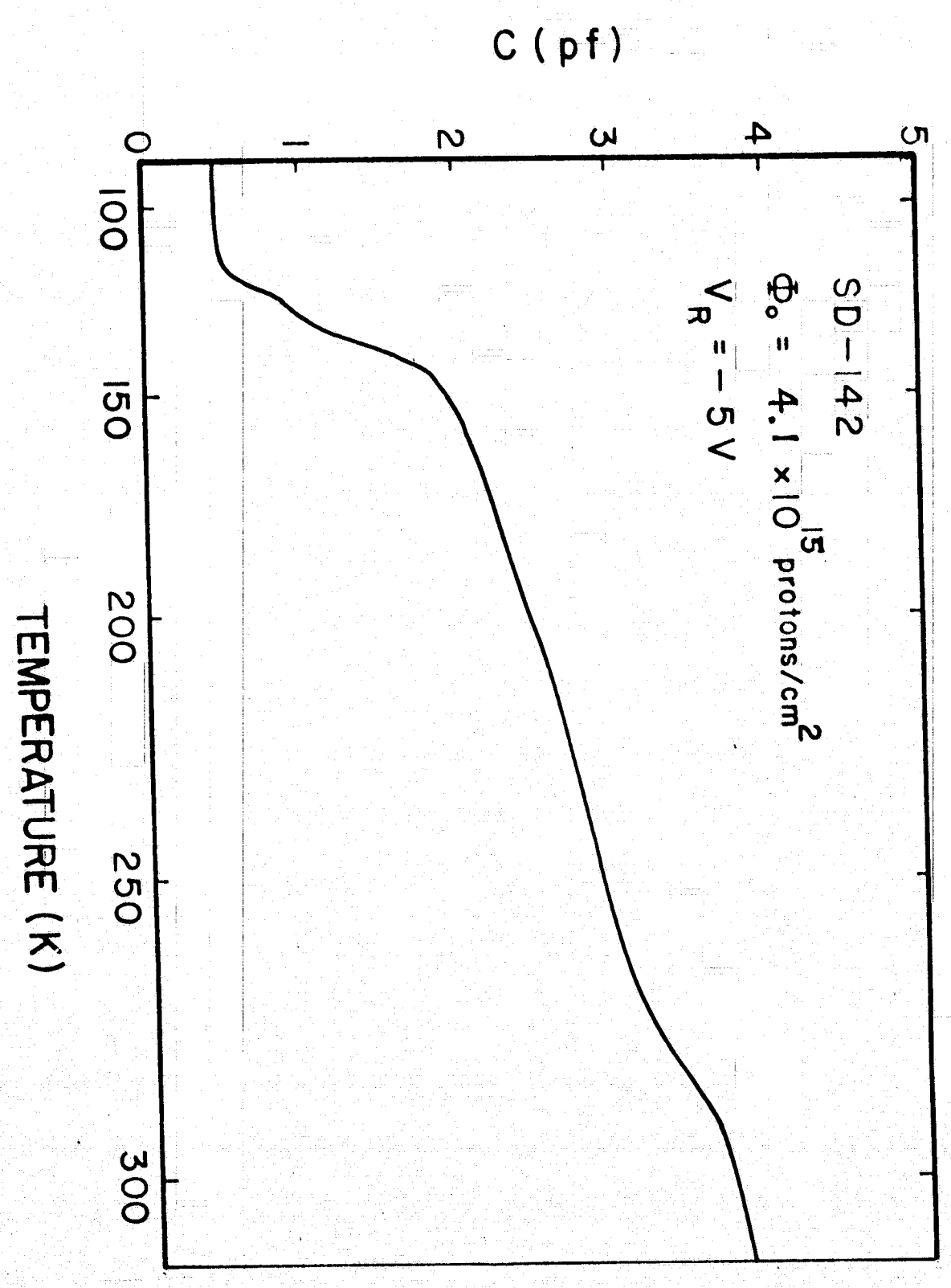

Fig. 14 The TSCAP scan of an one- MeV proton irradiated n-GaAs Schottky diode. Three capacitance steps were observed in this sample.

From the results shown in Fig. 11 through Fig. 14, it is interesting to note that sample SD-233, which has the lowest proton fluence, has produced the largest radiation induced defect density observed among the four irradiated diodes, as will be shown later. This, along with the results of I-V data shown previously as well as the DLTS data to be discussed later clearly illustrated that diode SD-233 has the highest radiation damage among all the proton-irradiated diodes studied in this work. One possible explanation of the result may be attributed to the fact that for diode SD-233, the depletion layer depth studied was around 3 to 4μm from the junction while it was about 6 to 18μm for the rest of the diodes with higher proton fluence. The fact that defect distribution and density observed at 3 to 4μm range for diode SD-233 could be significantly different from those at 6 to 18μm depth observed in other irradiated diodes. Detailed study of the spatial dependence of the trap densities in these diodes is currently in progress and the results will be discussed in the next technical report.

3.4 Results of the DLTS Measurements

The deep-level transient spectroscopy (DLTS) measurement technique developed by Lang [4] provides a fast thermal scan of all the defect levels which are electrical active in a p-n junction or a Schottky barrier diode. Because of higher signical frequency (20~50 MHz) than the classical TSCAP method (1 MHz), the DLTS technique has proven to be a more sensitive and useful experimental tool than the TSCAP method for defect characterization.

The main feature of the DLTS measurement technique lies in its ability to set an emission rate window such that the measurement apparatus only responds when it sees a transient with an emission rate within this

window. Thus, if the emission rate of a trap is varied by changing the sample temperature, the instrument will show a response peak at the temperature where the trap emission rate is within the window. The electron emission rates are thermally activated and can be expressed by [4]

$$e_n = \sigma_n \langle v_n \rangle N_c \exp(-\Delta E/k_o T) \tag{8}$$

where σ_n is the electron capture cross section, $\langle v_n \rangle$ is the mean thermal velocity, N_c is the effective density of the conduction band states, and ΔE is the thermal activation energy of the defect level (i.e., $\Delta E = E_c - E_t$ for electron traps).

For n-type GaAs, the mean thermal velocity is given by

$$\langle v_n \rangle = (3kT/m_n^*)^{1/2}$$

$$= 2.3 \times 10^6 \, T^{1/2} \text{ cm/s} \tag{9}$$

where $m_n^* = 0.086 \, m_o$ is the electron effective mass in GaAs material.

The characteristic capacitance transient from each energy level may be detected by measuring the transient as a function of temperature. This transient may be measured using a signal averager, or more conveniently the DLTS experiments by Lang [4]. A measurement of the initial values of the transient capacitance versus temperature using a two channel Box Car averager produces a trap energy spectrum. If a single level trap emission is predominant at a particular temperature, which is frequently the case when two traps are far apart, then one normally obtains a spectrum having distinct peaks. For such a case, the initial values of the transient capacitance $\Delta C(0)$ can be obtained from an emission peak of a given energy level at a given temperature as [4]

$$S(\tau) = \Delta C(0)(e^{-t_1/\tau} - e^{-t_2/\tau}) \tag{10}$$

where $S(\tau)$ is the emission peak from the output signal of a Box Car averager; t_1 and t_2 are the time setting for the two channels in the instrument, respectively, and τ is emission time constant of the given level as described in eq. (8). The thermal activation energy, ΔE, of a given trap level may be calculated from the Arrhenius plot obtained from a series of temperature measurements of $S(\tau)$ using different t_1 and t_2 values.

The electron thermal emission rate, e_n, corresponding to the maximum peak of DLTS signal is a precisely defined quantity and may be calculated from the following expression:

$$e_n = \tau_m^{-1} = \ell n(t_1/t_2)/(t_1-t_2) \tag{11}$$

Equation (11) is obtained from differentiating eq. (10) with respect to τ, namely,

$$\left.\frac{dS(\tau)}{d\tau}\right|_{\tau_{max}} = 0 \tag{12}$$

We shall next discuss the experimental results obtained from the DLTS measurements on both unirradiated and one-MeV proton irradiated n-GaAs Schottky barrier diodes. Information such as defect energy levels and densities, thermal emission and capture rates at each trap level is deduced from the DLTS measurements.

(i) Defect Energy Levels and Thermal Emission Rates

We shall first discuss the energy levels and the thermal emission rates for the electron traps deduced from the DLTS measurements in both

unirradiated and proton-irradiated n-GaAs Schottky diodes. Figure 15 shows a DLTS thermal scan for an unirradiated GaAs Schottky diode, SD-234. In this plot, three distinct emission peaks corresponding to three electron traps in the upper half of the band gap are observed in this sample. The thermal activation energy for each defect level was obtained from a series of DLTS scans with different rate windows (i.e., with different t_1 and t_2 settings), as described previously. From the thermal emission rates versus inverse temperature plot yields the thermal activation energies for the three electron traps, which are given respectively by $E_2 = 0.38\pm0.02$ eV, $E_4 = 0.65\pm0.02$ eV, and $E_5 = 0.78\pm0.02$ eV, below the conduction band edge, E_c. These values do not include the T^2 correction in the calculation. Figure 16 shows a series of DLTS thermal scans with different rate windows for another unirradiated diode, SD-231. It is interesting to note that an additional electron trap at $E_1 = 0.17\pm0.01$ eV below E_c was observed in this sample. This defect level may be related to the gallium vacancy as being reported by Chang et al. [11]. The E_5 electron trap can be attributed to the oxygen donor level in GaAs [10,12]. Chang et al. [11] have also observed an oxygen-vacancy complex with $\Delta E = E_c - 0.32$ eV. This defect level is similar to the E_2 level observed in our GaAs Schottky diodes. However, it is worth to point out that exact identification of the physical origin of these defects is extremely difficult by simply using the DLTS measurement technique. However, a combination of the DLTS method with structure analysis and other measurement techniques may help to resolve this dilemma. The DLTS spectra for the proton-irradiated devices are shown in Fig. 17 through Fig. 20. Figure 17 shows the DLTS scan for diode SD-233 with $\phi_o = 5.8\times10^{12}$ cm^{-2}. In this diode, five main electron traps and two

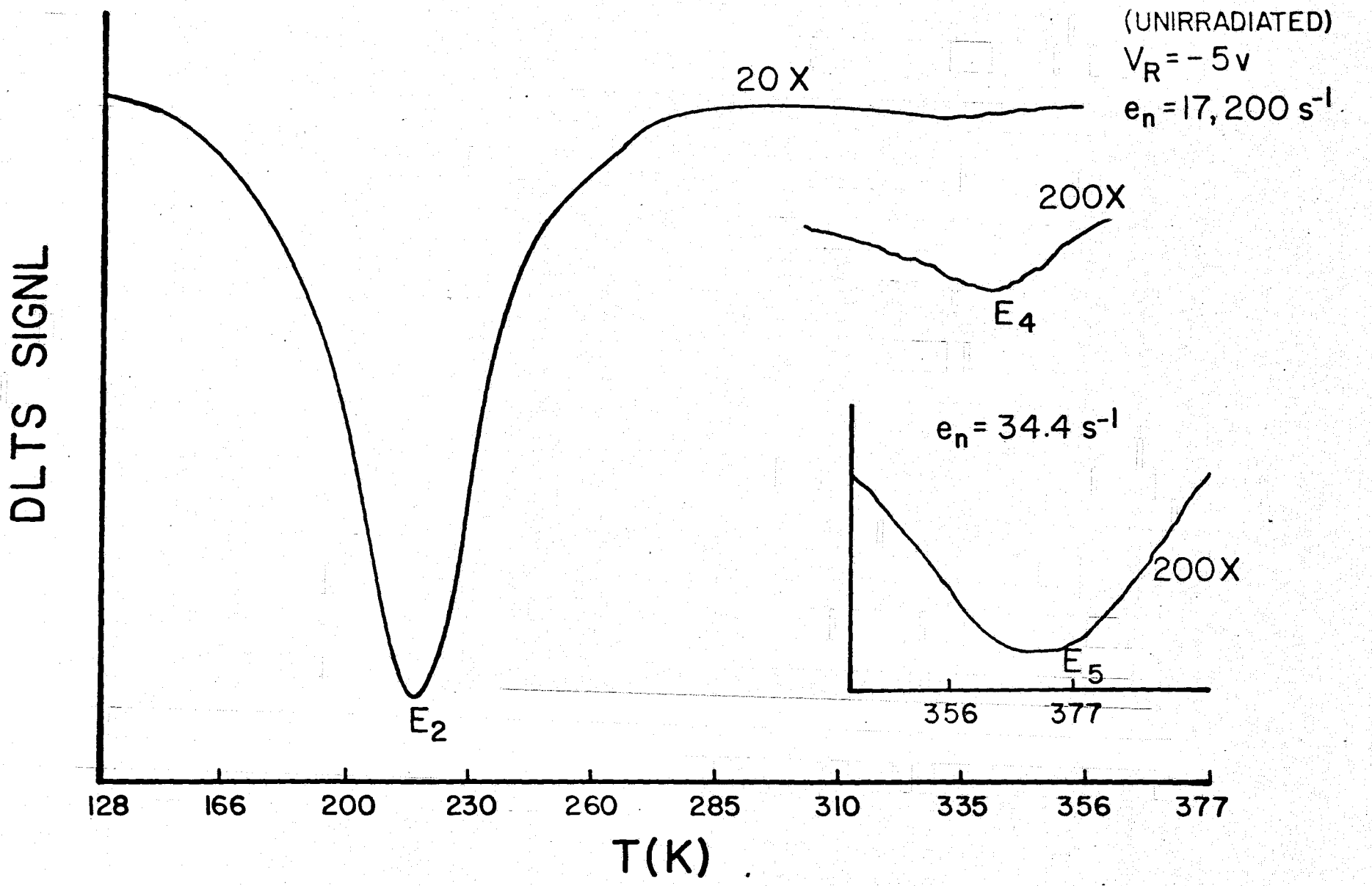

Fig. 15 The DLTS thermal scan of an unirradiated n-type GaAs Schottky barrier diode. Three electron traps were observed in this sample.

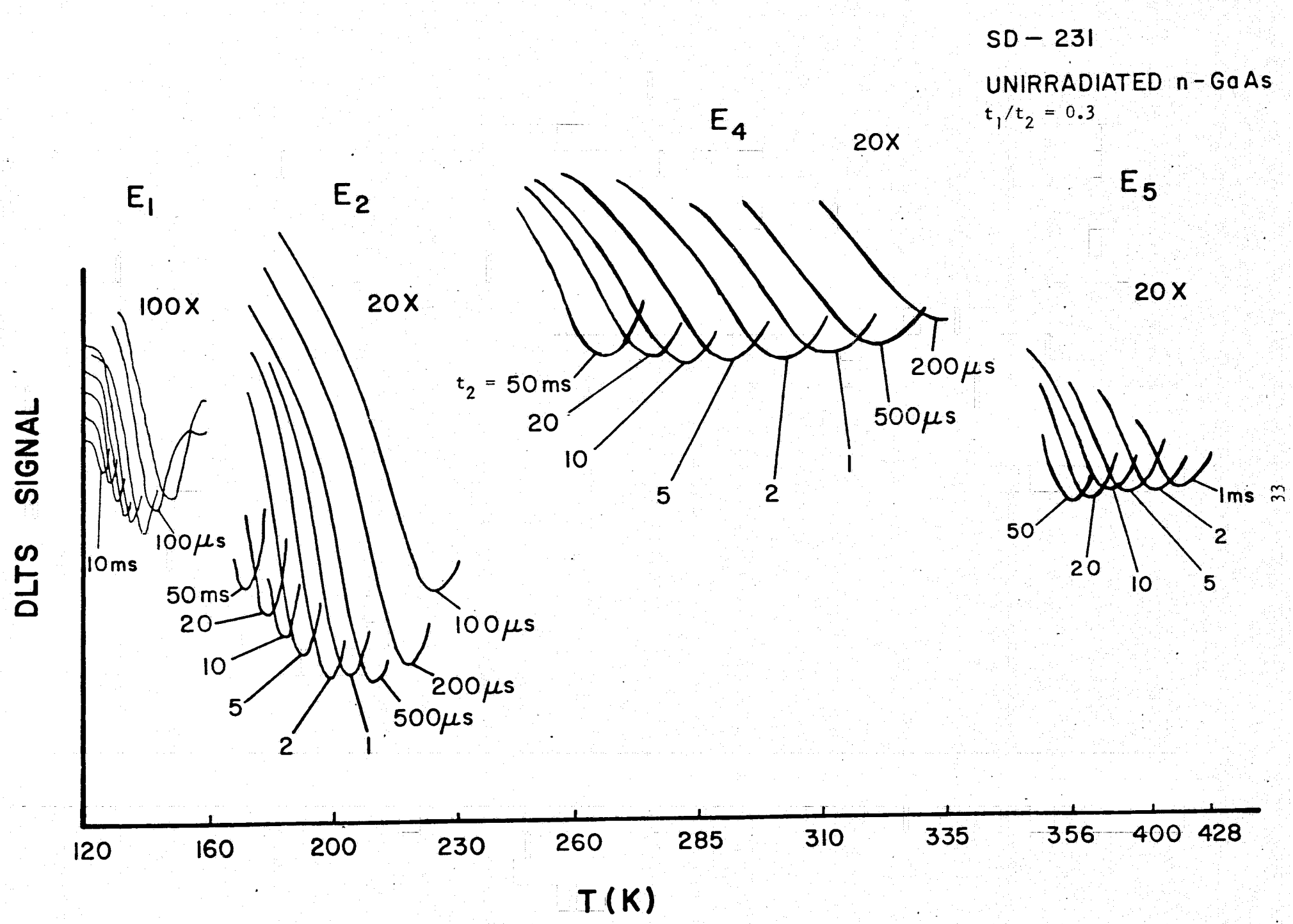

Fig. 16 The DLTS thermal scan of an un-irradiated n-type GaAs Schottky diode. Four electron tra[illegible] were [illegible] thi[illegible] ampl[illegible] The [illegible] fer[illegible] rat[illegible] indo[illegible] shown allowed the [illegible] calculation

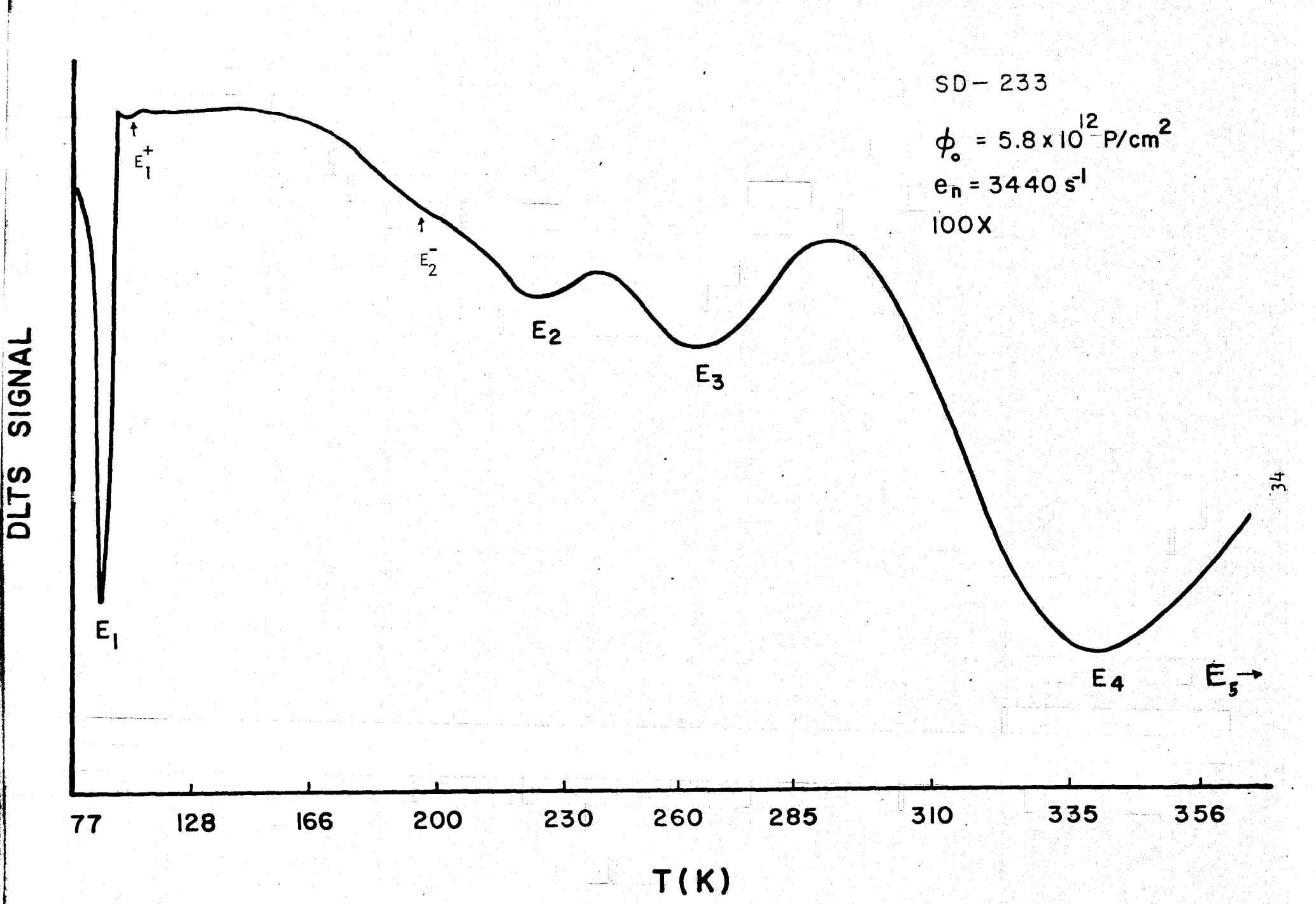

Fig. 17 The DLTS thermal scan of an one-MeV proton irradiated n-GaAs Schottky diode. Only four electron traps were shown; the fifth electron trap level (E_5) was not shown in the figure.

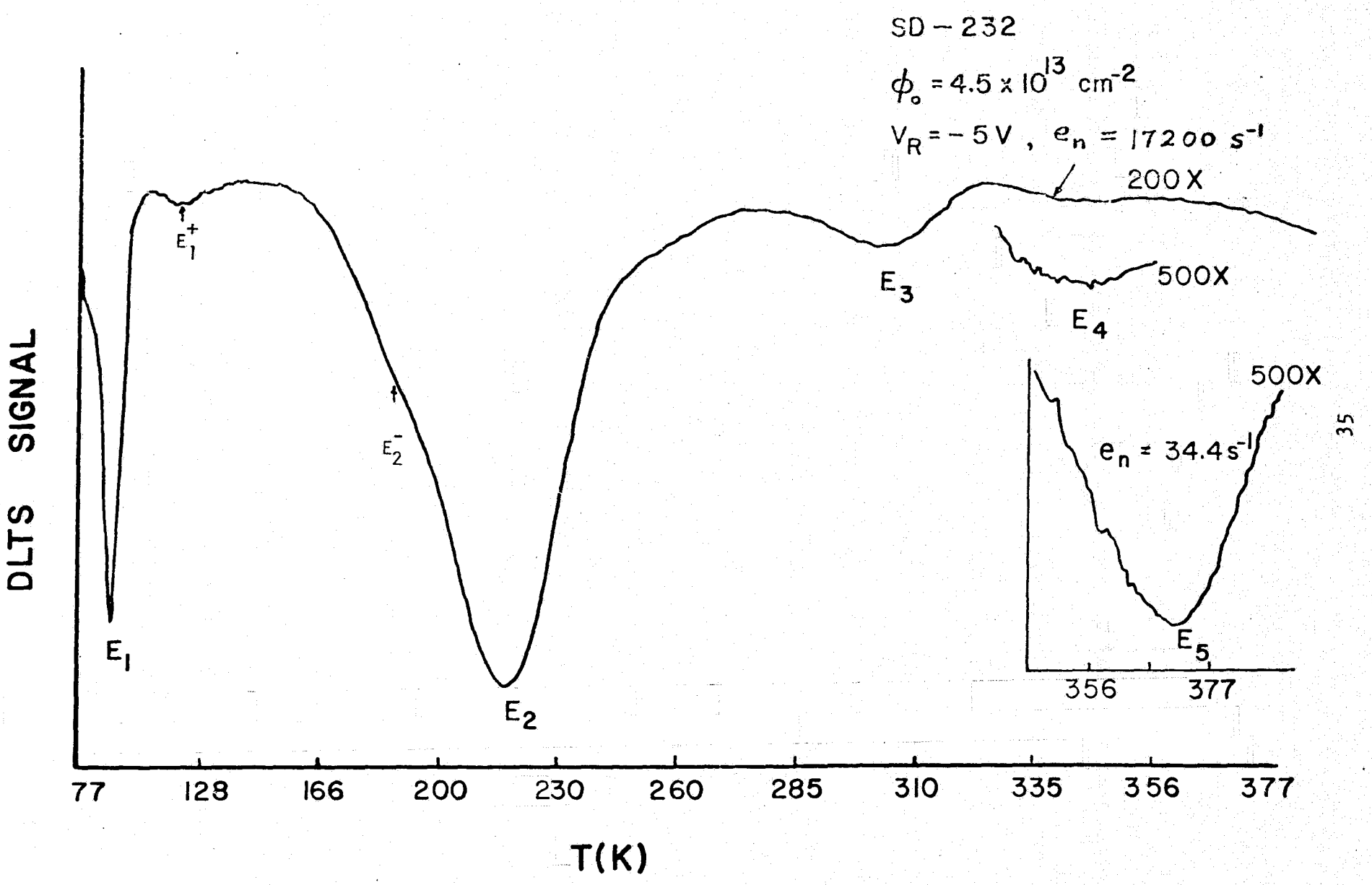

Fig. 18 The DLTS thermal scan of an one-MeV proton irradiated n-GaAs Schottky barrier diode. Five lectron traps were detected in this sample.

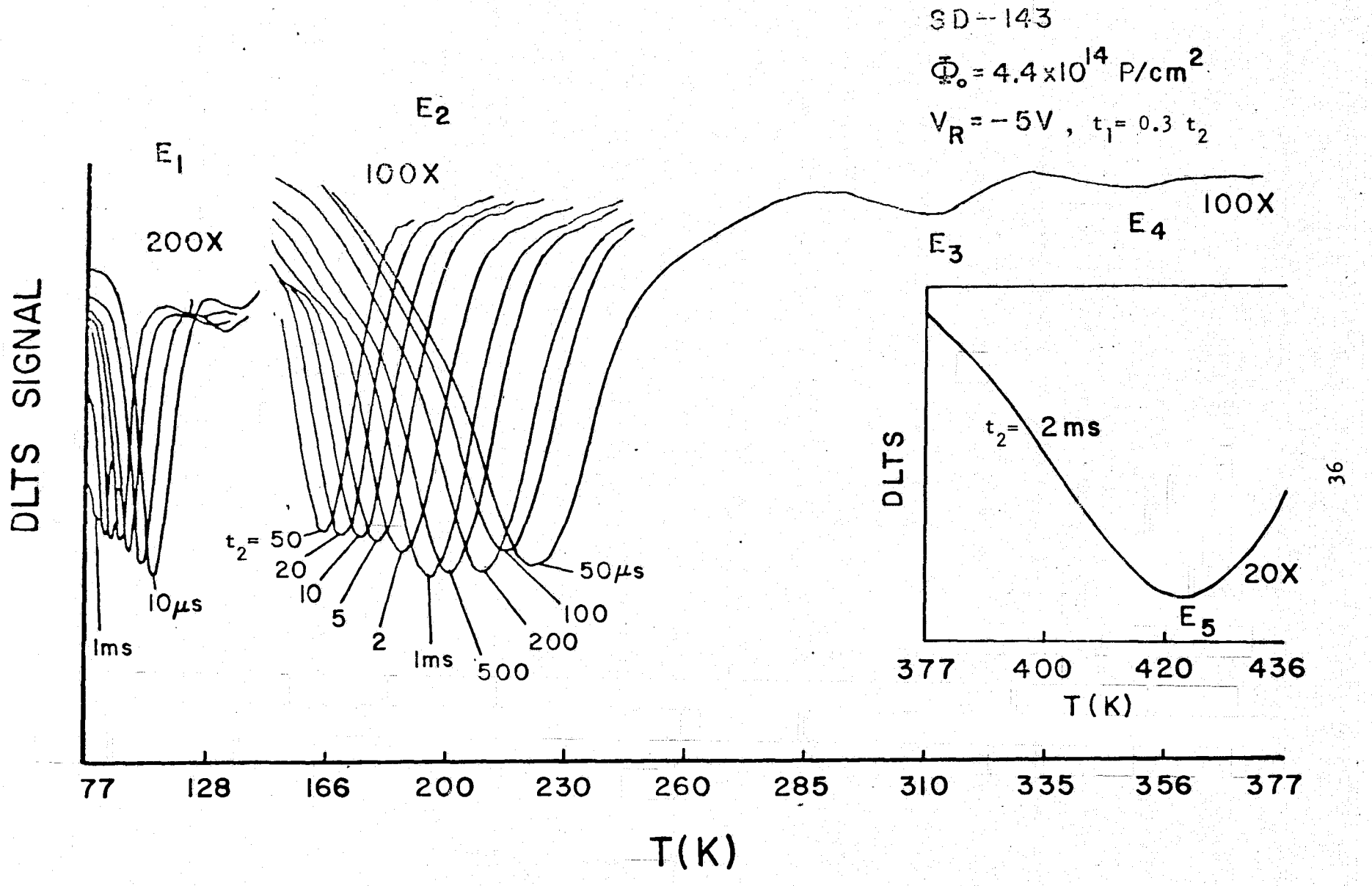

Fig. 19 The DLTS thermal scan of an one-MeV proton irradiated n-GaAs Schottky barrier diode, with different rate windows. Five main electron traps were observed in this sample.

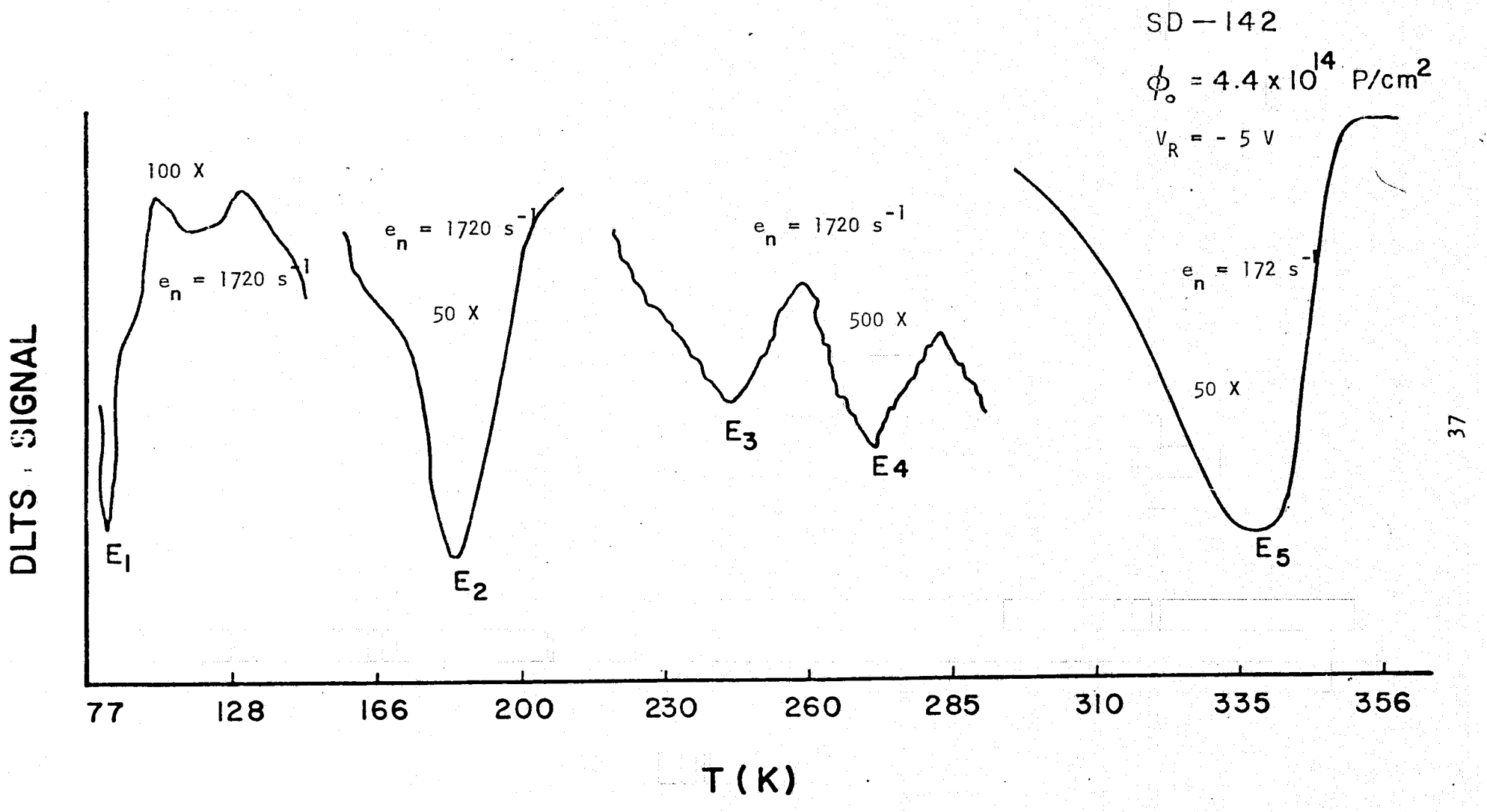

Fig. 20 The DLTS thermal scan of an one-MeV proton irradiated n-GaAs Schottky barrier diode. Five electron traps were detected in this sample.

small satellite levels were observed in the DLTS thermal scan for 77<T<450K. This includes three defect levels (i.e., E_2, E_4, and E_5) which are identical to those observed in the unirradiated diodes and two proton-induced defect levels $E_1 = E_c - 0.14$ eV, and $E_3 = E_c - 0.46$eV. The two small satellite levels are given respectively by $E_1^+ = E_c - 0.19$ eV, and $E_2^- = E_c - 0.29$ eV. Figure 18 through Fig. 20 display the DLTS spectra for three other proton-irradiated diodes SD-232, -143, and -142 with incremental proton fluence (i.e., ϕ_o from 4.5×10^{13} to 4.1×10^{15} cm^{-2}). The results yield identical defect levels as that observed in the irradiated diode SD-233. However, it was found that level E_3 has a thermal activation energy which varies with proton fluence (i.e., $E_3 = E_c - 0.51$ eV for SD-232 and increases to $E_c - 0.60$ eV for SD-142; see Fig. 23) while thermal activation energy for other defect levels remains unchanged. The reason for the E_3 level to shift towards higher energy may be attributed to the fact that the interaction between defect levels E_3 and E_4 appears to intensify as proton fluence increases from 5.8×10^{12} to 4.1×10^{15} cm^{-2}. This is clearly demonstrated in Fig. 21 in which the DLTS signal for level E_3 was found to increase with increasing proton fluence. The merging of these two defect levels at higher proton fluence is also clearly illustrated in this plot.

As mentioned previously, the electron thermal emission rates for each defect level can be determined from a series of DLTS thermal scans, as shown in Fig. 16 and Fig. 19. The results of these emission rate measurements are displayed in Fig. 22, along with the calculated thermal activation energy for each defect level. These defect levels represent electron traps located in the upper half of the band gap. Defect levels E_2, E_4, and E_5 are due to the intrinsic defects observed in all n-GaAs

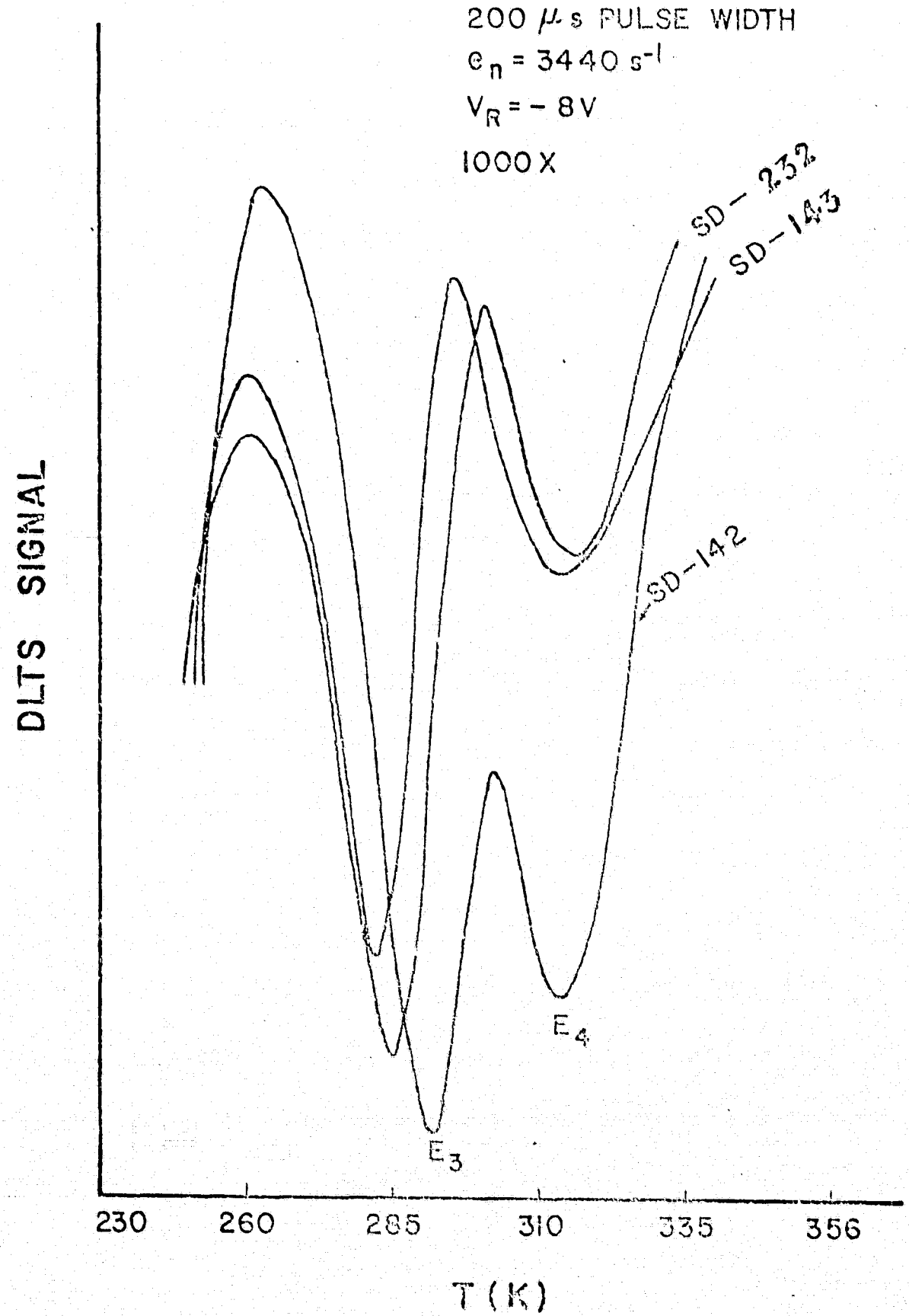

Fig. 21 The DLTS spectra of defect levels E_3 and E_4 as a function of proton fluence for samples SD- 232, 143, qnd 142.

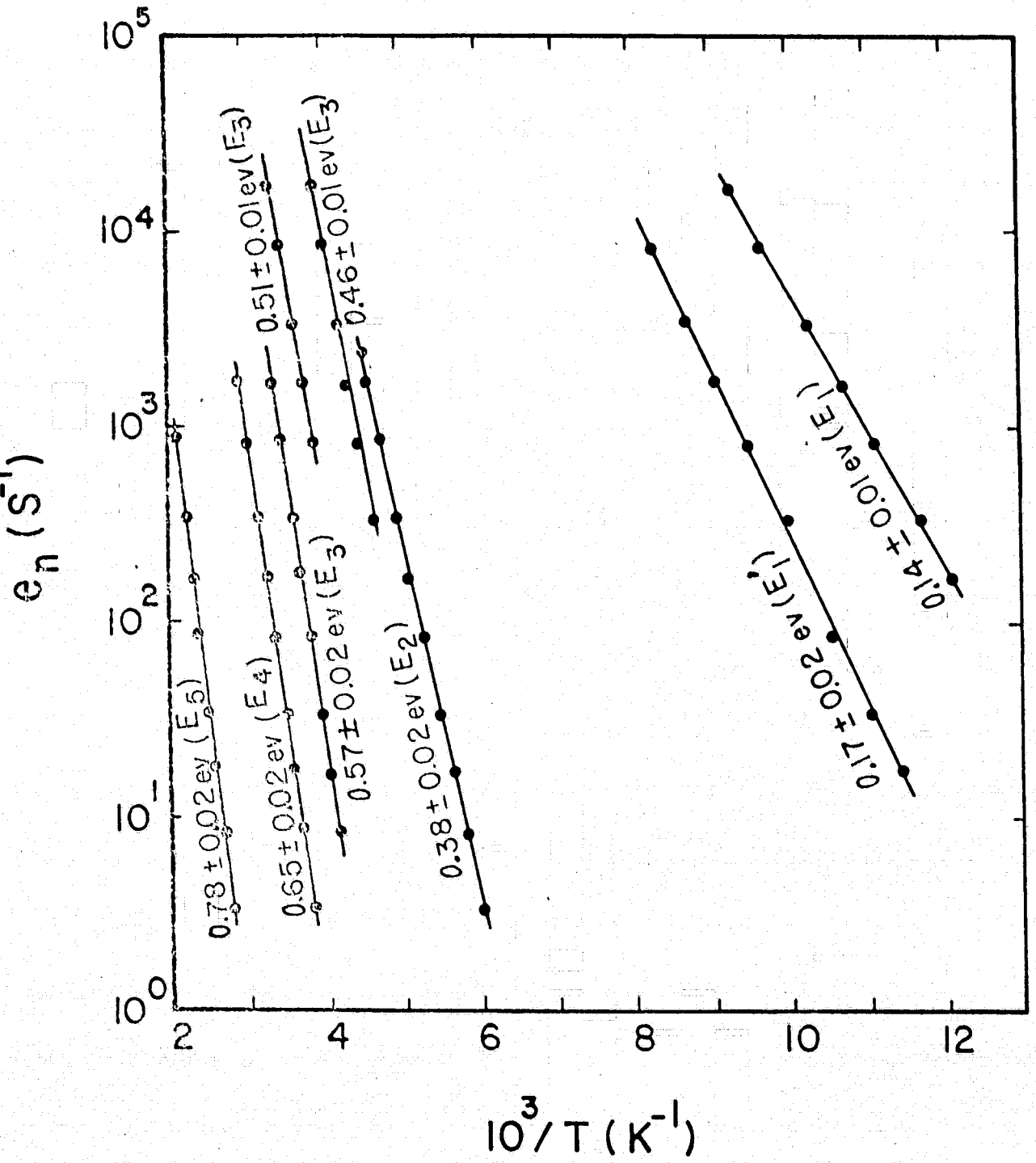

Fig. 22 Thermal emission rates of electrons veresus reciprocal temperature for the un-irradiated and one-MeV proton irradiated n-GaAs Schottky diodes (i.e.,. two unirradiated and four irradiated diodes).

diodes studied, while level E_1' is only observed in the unirradiated diode SD-231, and levèls E_1 and E_3 are only observed in the proton-irradiated diodes. Figure 23 shows the energy level diagram for all the defect levels observed in this work for both unirradiated and one-MeV proton irradiated n-GaAs diodes. The measured defect energy levels, majority carrier density, as well as the proton fluence used in each sample are listed in Table I.

In order to compare our measured defect levels in proton-irradiated n-GaAs with those published previously, we surveyed all the defect levels reported by previous investigators as induced by different irradiation sources. The results are listed in Table II, along with the methods they used in determining these energy levels. From this table, it is obvious that proton-induced defect level E_1 observed in this work has also been reported by Aukerman and others [13,15,17] in the electron-irradiated GaAs samples. The fact that this level observed in n-GaAs bombarded by different irradiation sources clearly indicates that this level is a vacancy related defect. To justify this statement we show in Fig. 24 the energy level diagram for vacancy associated defects in annealed GaAs as reported by Chang et al. [11] from cathodoluminescence measurements at 5K. They observed an arsenic vacancy defect level at $E_c - 0.14$ eV, which is identical to our proton induced-defect level E_1. A further comparison of our results with those of Chang's indicates that our E_1^+ and E_4 defect levels may be due to gallium vacancies. The proton induced defect level E_3 observed in this work is also believed to be a vacancy related defect. Several investigators [14,19,20,22] have also reported defect levels with energies lying between 0.45 to 0.6 eV below the conduction band. Finally, the defect level $E_5 = E_c - 0.78$ eV

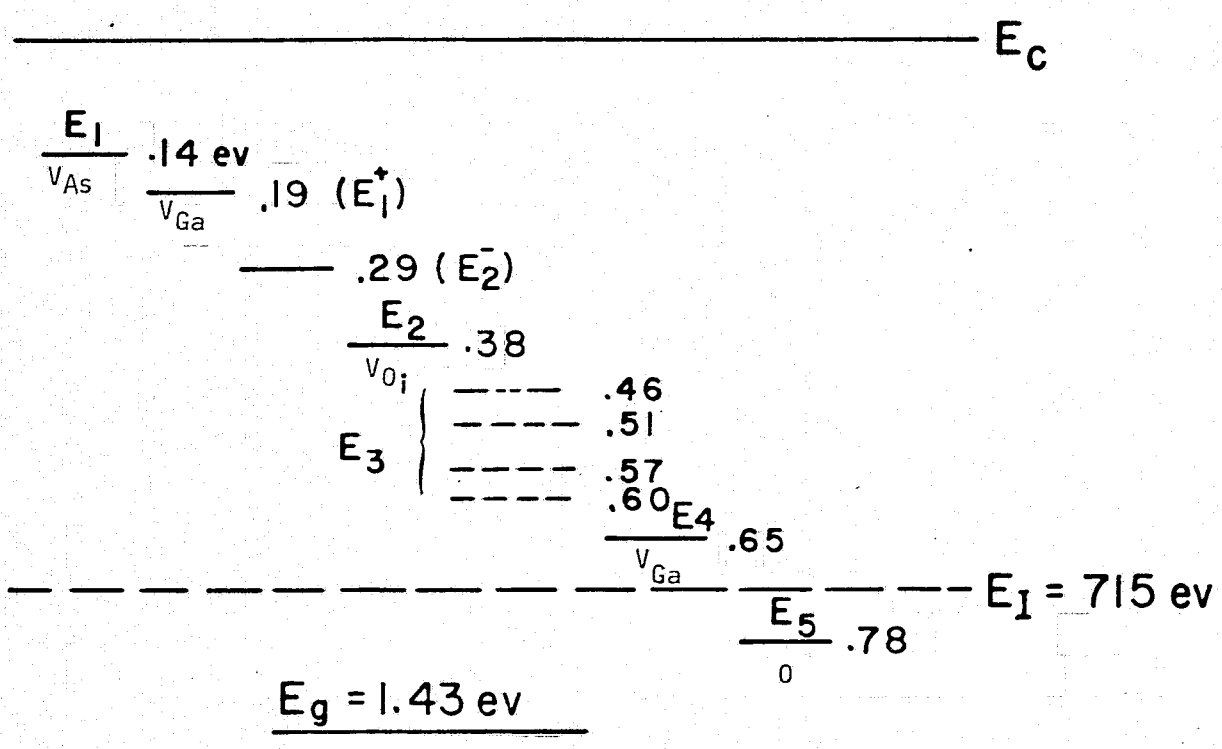

Fig. 23 The measured thermal activation energy of the unirradiated and one- Mev proton irradiated n-GaAs Schottky barrier samples. Figure shows five main electron traps (E_1 through E_5) and two satellite levels (E_1^+ and E_2^-) along with the reported gallium and arsenic vacancy defect levels.

Table I Energy levels (electron traps) and proton fluence for one-MeV proton irradiated n-type GaAs

Energy levels (eV)* / Test Samples	E_1	E_2	E_3	E_4	E_5	Proton fluence (P/cm^2)	$(N_D-N_A)^{\dagger}$ cm^{-3}
SD-231	0.17±0.02 (0.15)	0.38±0.02 (0.33)	-	0.65±0.02 (0.60)	0.78±0.02 (0.71)	unirradiated	$\sim 2.2\times10^{16}$
SD-234	-	0.38±0.02	-	0.65±0.02	0.78±0.02	unirradiated	$\sim 1.7\times10^{16}$
SD-233	0.14±0.01 (0.13)	0.38±0.02	0.46±0.01 (0.41)	0.65±0.02	0.78±0.02	$\phi_o=5.8\times10^{12}$	$\sim 7.9\times10^{14}$
SD-232	0.14±0.01	0.38±0.02	0.51±0.01 (0.46)	0.65±0.02	0.78±0.02	4.5×10^{13}	$\sim 4.8\times10^{14}$
SD-143	0.14±0.01	0.38±0.02	0.57±0.02 (0.54)	0.65±0.02	0.78±0.02	4.4×10^{14}	$\sim 4.2\times10^{14}$
SD-142	0.14±0.01	0.38±0.02	0.60±0.01 (0.57)	0.65±0.02	0.78±0.02	4.1×10^{15}	$\sim 4.0\ 10^{14}$

* Energy levels were measured from the conduction band edge; the values given in parenthesis taken into account the T^2 correction in Eq. (9) as discussed in the text.

† Background concentration (N_D-N_A) as determined from C-V measurements.

Table II Defect energy levels induced by various irradiation sources in GaAs

Defect Energy Level	Irradiation Source	Method Used	References
E_c - 0.13 eV	950 KeV electrons at 300K	Hall effect	Auberman and Graft [13]
E_c - 0.1 eV E_c - 0.5 eV E_c - 0.6 eV	fast neutron at 10^3 n/cm^2-S at 100C	Hall effect	Auberman et al. [14]
E_c - 0.14 eV	2 MeV electrons at 80K	Hall effect	Stein [15]
E_c - 0.13 eV E_c - 0.16 eV E_c - 0.30 eV E_c + 0.10 eV E_v + 0.059 eV	1.25 MeV 60 Co γ rays at 300K	Hall effect	Brehm and Pearson [16]
E_c - 0.02 E_c - 0.15 } n-type E_v + 0.17 E_v + 0.06 } Zn-doped	1 MeV electron (at 30°C)	Hall effect	Kalma and Berger [17,18]
E_c - 0.5 eV E_c - 1.0 eV	20 MeV H^{++} and 2 MeV electron at 50°C	Infrared attenuation spectrum	Brundnyi et al. [19]
E_c - 0.54 eV E_v + 0.11 eV	0.8 MeV electrons at 300K	Infrared photo-conductivity	O'Brien and Corelli [20]
E_v + 0.8 eV E_v + 0.4 eV	25 KeV proton	temperature dependent conductivity	Pruniax et al. [21]
E_c - 0.08 eV E_c - 0.19 eV E_c - 0.45 eV E_c - 0.76 eV E_c - 0.96 eV E_v + 0.76 eV E_v + 0.44 eV E_v + 0.32 eV	1 MeV (e^-) 600 KeV (P^+) 1.8 MeV (He^+) 185 KeV (O^+) at 300K	DLTS	Lang and Kimerling [22], Kimerling et al. [23]

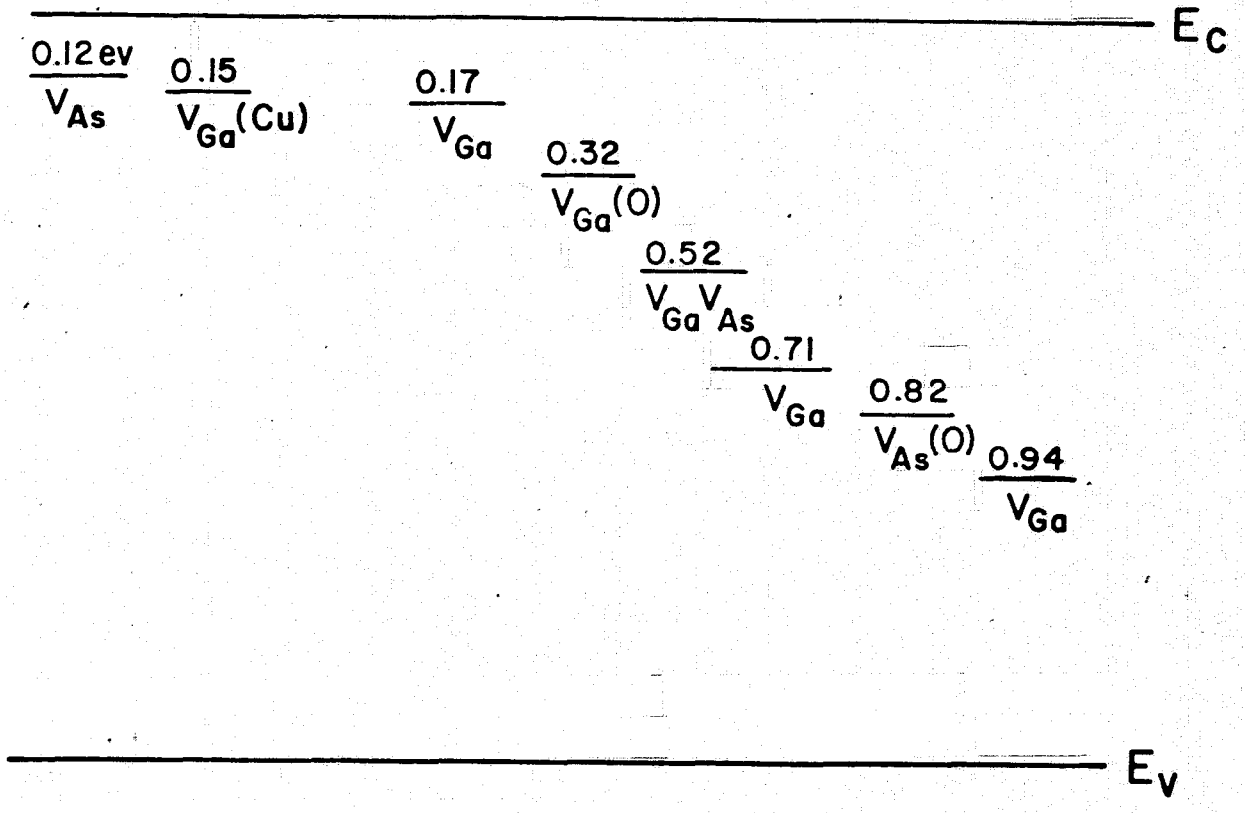

Fig. 24 Energy levels associated with gallium and arsenic vacancies in GaAs as determined by the cathodoluminescence spectra at 5 K (Chang et al., Appl. Phys. Lett., 19, 143 (1971).

reported in this work has also been reported by Kimerling et al. [23] in the 185 KeV (0^+) implanted GaAs samples. We have attributed this defect level to an oxygen donor level [11,12].

(ii) Electron Capture Cross Section

The thermal capture cross section of electrons in each electron trap may be determined by varying the pulse width in the DLTS thermal scans. If we assumed that the capture process is dominant, and $N_T(t)$, $N_T(\infty)$ are the density of electron trap at time t and ∞, respectively, then $N_T(t)$ can be expressed by:

$$N_T(t) = N_T(\infty)\ [1 - \exp(-t/\tau_c)] \tag{13}$$

where

τ_c is the capture time constant which is related to the electron density, n_o, mean thermal velocity, v_n, and electron capture cross section, σ_n, by

$$\tau_c = \frac{1}{n_o\ v_n\ \sigma_n} \tag{14}$$

Here we assume that capture time constant is much shorter than the emission and recombination time constants. By substituting eq. (14) into eq. (13) and solving for σ_n yields:

$$\sigma_n = \left(\frac{1}{n_o v_n}\right) \cdot \frac{d\ell n\left[1 - \frac{N_T}{N_T(\infty)}\right]}{dt} \tag{15}$$

Thus, the electron capture cross section, σ_n, can be determined from the plot of $\ell n[1 - \frac{N_T}{N_t(\infty)}]$ vs. t (i.e., the pulse width), while values of

$[1 - \frac{N_T(\infty)}{N_T}]$ are directly proportional to the magnitude of DLTS peaks at different pulse widths.

Figure 25 through Fig. 27 show the DLTS thermal scans as a function of the pulse width for two proton-irradiated diodes, SD-142 and SD-232, respectively. From these plots and with the help of eq. (15) we calculated the electron capture cross sections in each defect level, and the results are summarized in Table III. Our results revealed that thermal capture cross sections of electrons in these defect levels have values ranging from 10^{-13} to 10^{-15} cm^2. To determine the type of these defect levels (i.e., donor or acceptor type) we performed the bias voltage dependent study of the DLTS thermal scans for different pulse widths. This is shown in Fig. 26 for defect level E_3 in which the bias voltages across the Schottky diode were varied in steps from -6 to -4V, -4 to -2V, and -2 to 0V. The field dependent of thermal capture cross section is detected by observing the DLTS peaks at different pulse widths. If there is a shift in the DLTS peaks with pulse widths at a fixed bias voltage, then this is an indication of the electric field dependent of the thermal capture cross section for this particular defect level. The slight shift in the DLTS peaks at different pulse widths shown in Fig. 26 for defect level E_3 is a clear indication of the field dependent of the capture cross section for this level. A similar study for other defect levels indicates that thermal capture cross sections for levels E_2, E_4, and E_5 are independent of electric field while level E_1 showing stronger field dependent. The results are illustrated in Fig. 28 for diode SD-232.

In view of the large capture cross sections of electrons observed and the field independent nature, it is obvious that levels E_2, E_4, and E_5 observed in this work for n-GaAs are donor type defect centers while proton-induced levels E_1 and E_3 are acceptors type defect centers.

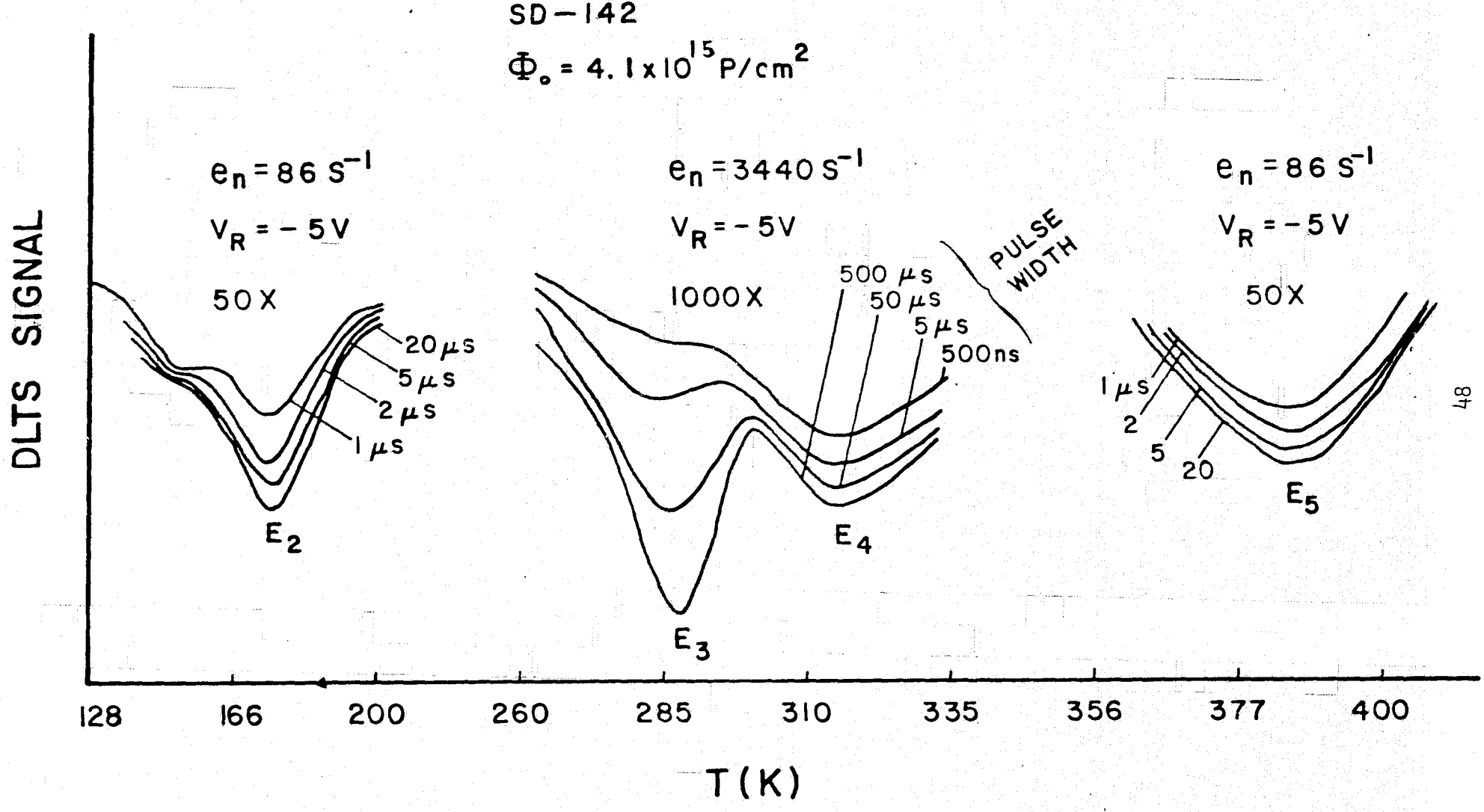

Fig. 25 DLTS scans for diode SD-142 as a function of pulsewidth for defect levels E_2, E_3, E_4, and E_5. The electron capture cross sections can be deduced from these spectra.

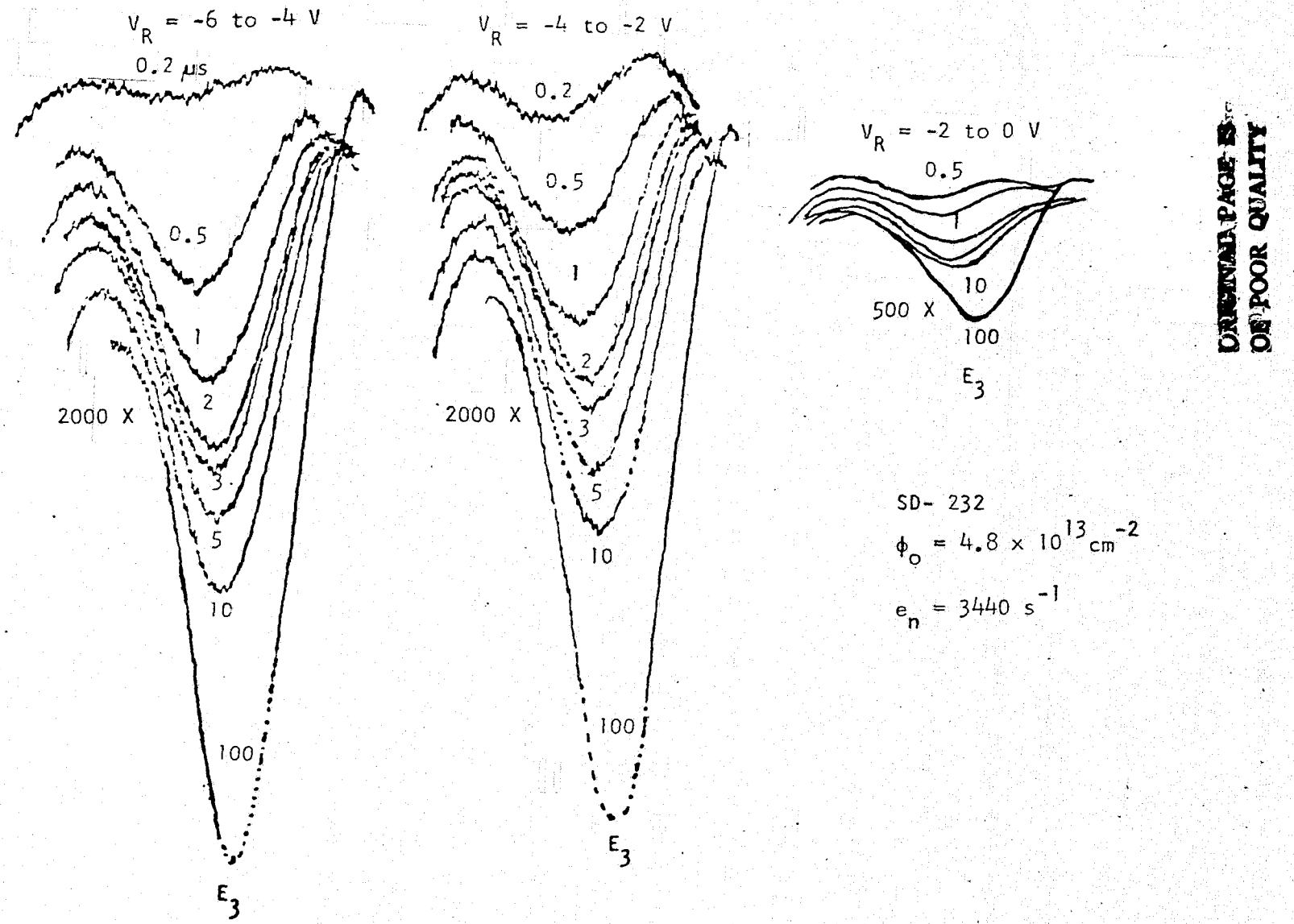

Fig. 26 The DLTS scans as a function of bias pulse width for different bias voltages for diode SD-232. The results show the field dependence of capture cross section for level E_3.

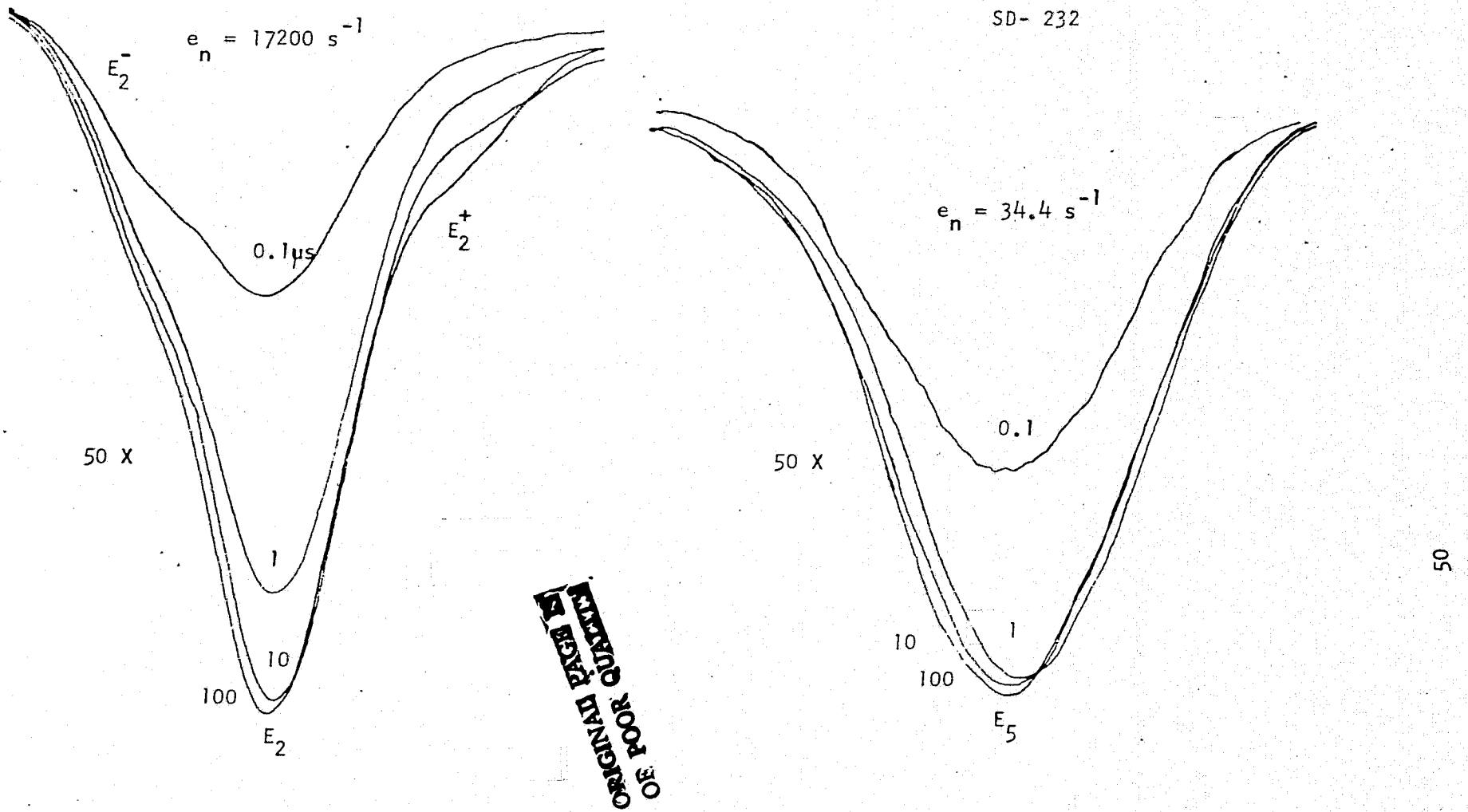

Fig. 27 The DLTS scans as a function of the bias pulse width for levels E_2 and E_5 For diode SD-232 with $\phi_o = 4.8 \times 10^{13}$ cm^{-2}. Electron capture cross section for both levels show little or no field dependence.

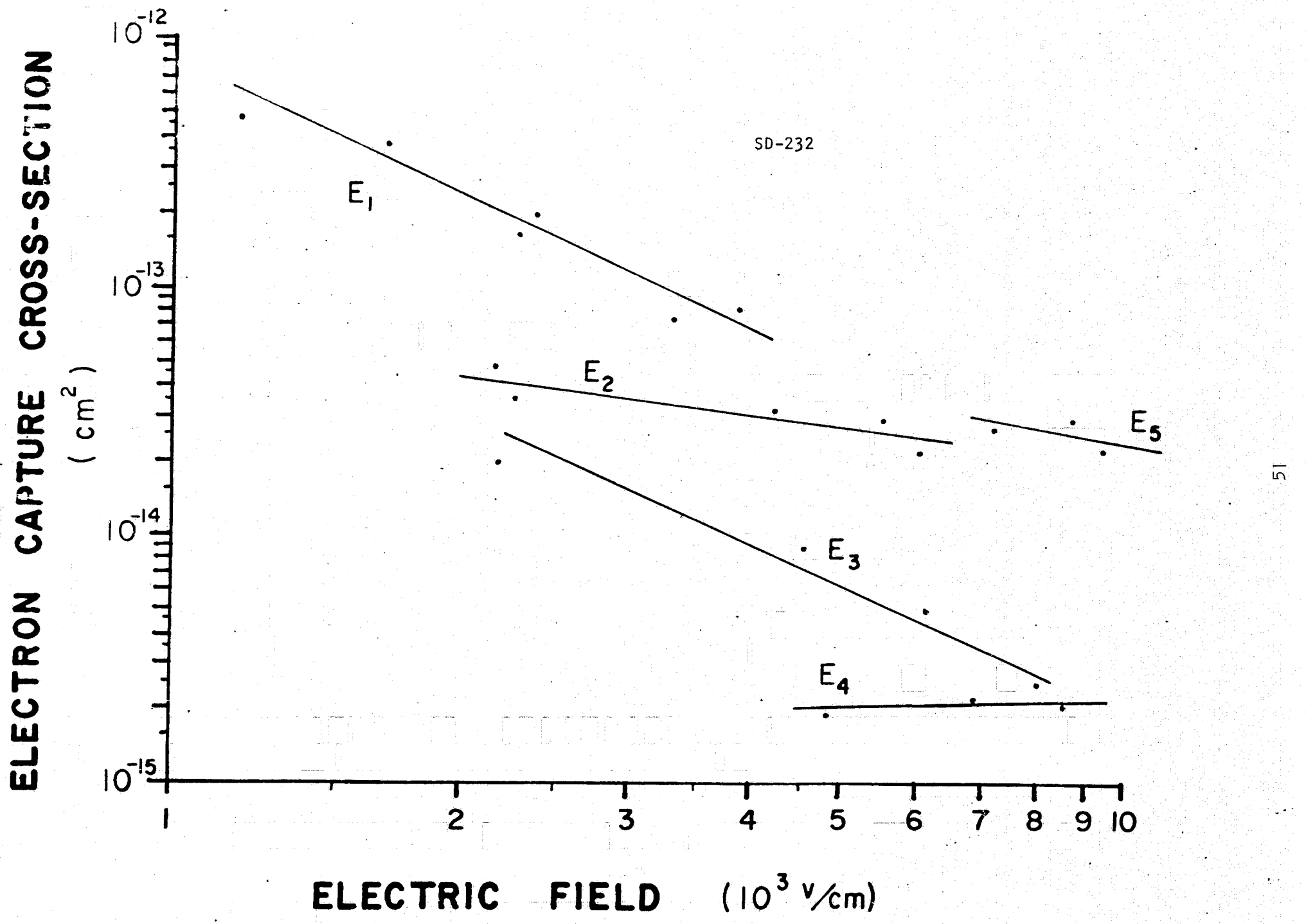

Fig. 28 Thermal capture cross section versus electric field for the five electron traps observed in diode SD-232.

Table III Thermal capture cross section (σ_n) of electrons in proton-irradiated nGaAs diodes SD-232 and SD-142

Energy levels	E_1	E_2	E_3	E_4	E_5
σ_n (cm^2) (SD-232)	4.87E-13	2.19E-14	7.35E-15	2.22E-15	1.88E-14
σ_n (cm^2) (SD-142)	2.38E-13	2.73E-14	5.28E-15	4.52E-15	1.07E-14

(iii) Defect Density

As discussed in the previous section, the density of each defect level can be determined by either using the TSCAP or the DLTS method based on eq. (7) provided that the assumptions made are satisfied (i.e., $N_T \leq 0.1\ N_D$, and N_T and N_D are constants throughout the depletion layer of the Schottky diode). In the course of the present study, we have discovered that the density of electron traps in the proton-irradiated GaAs Schottky diodes may be spatial dependent. Thus, it is necessary to determine the density of traps by applying a small incremental bias voltage (i.e., 0 to -2V, -2 to -4V, -4 to -6V, etc.) across the Schottky barrier diode and observe the change in capacitance due to electron emission from the specific trap level. Using this method, it is possible to deduce the spatial dependence of each trap level density in n-GaAs Schottky barrier diodes. As an example, the measured capacitance change from capacitance transient measurements for several one-MeV proton irradiated n-GaAs Schottky diodes is illustrated in Fig. 29. It is noted that the magnitude of the capacitance change is directly proportional to the trap density in each defect level. The results show that diode SD-233 has the largest defect density when compared with other irradiated diodes.

The calculated defect densities for all electron traps in diode SD-233 are listed in Table IV, along with the measured values of capacitance steps shown in the TSCAP plot. The values of defect density listed in Table IV were computed from eq. (7) using the TSCAP data shown in Fig. 12 for diode SD-233. Note that the two proton-induced defect levels (i.e., E_1 and E_3) have the lower densities of defects when compared with the three other intrinsic defect levels (i.e., E_2, E_4, and E_5).

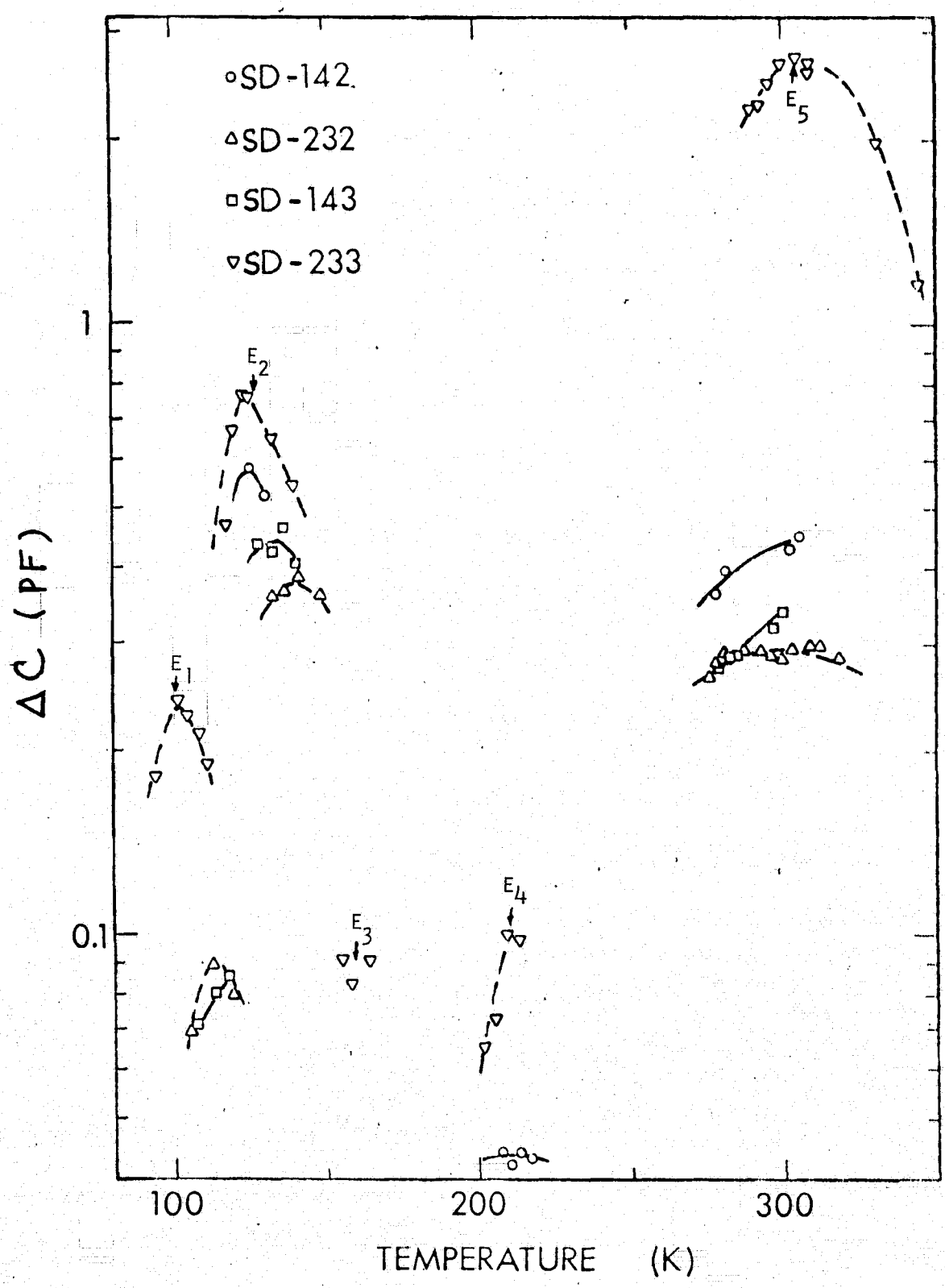

Fig.29 The observed capacitance change in each defect level as deduced from transient capacitance measurements for four proton- irradiated n-GaAs Schottky diodes.

Table IV Defect density in one-MeV proton-irradiated n-GaAs Schottky diode with $\phi_o = 5.8 \times 10^{12}$ cm^{-2} as determined from the TSCAP plot and eq. (7).

Energy levels	$\Delta C/C_o$	(N_D-N_A) cm^{-3}	$N_T(cm^{-3})$
E_1	0.058	2×10^{13}	2.3×10^{12}
E_2	0.173	9.6×10^{13}	3.3×10^{13}
E_3	0.015	1.3×10^{14}	3.9×10^{12}
E_4	0.016	1.8×10^{14}	5.7×10^{12}
E_5	0.2	8.2×10^{14}	3.3×10^{14}

It is important to point out that the above calculations were based on the assumption that the defect density is constant across the substrate, which may not be the case for the proton-irradiated GaAs. A more detailed analysis of the spatial dependence of trap density in proton-irradiated GaAs using the DLTS method is currently being undertaken, and the results of this work will be described in a future technical report.

IV. SUMMARY

From the results presented in this report, it is clear that the TSCAP and DLTS experiments are sensitive and useful experimental tools for defect characterization in semiconductors. Applications of these measurement techniques to study defect properties in one-MeV proton irradiated n-GaAs Schottky barrier diodes enable us to identify all the electron traps in the upper part of the band gap and to determine defect parameters associated with these electron traps. Good correlations have also been obtainedbetweenthe measured recombination-generation current and the defect parameters in n-GaAs Schottky diodes with and without proton irradiation. The main research findings during this research period are summarized as follows:

(i) From I-V data, it is found that the reverse saturation current and forward bias recombination current increase with increasing proton fluence for $\phi_o \geq 10^{13}$ cm^{-2}. While diode SD-233 with $\phi_o \simeq 5.8 \times 10^{12}$ cm^{-2} shows the highest radiation damage, its reverse saturation current increases by more than two orders of magnitude over that of unirradiated diode SD-234.

(ii) From C-V data, it is found that the majority carrier density (i.e., electrons) reduces by more than one order of magnitude as a result of the one-MeV proton irradiation in n-GaAs when ϕ_o is greater than 10^{13} cm^{-2}.

(iii) From the results of DLTS experiments, it is found that proton irradiation on n-type GaAs introduces new defect levels in the upper half of the band gap. Five main electron traps and two small satellite defect levels were observed in the proton-irradiated samples, while only three electron traps were detected in the unirradiated GaAs samples. The electronic properties of these defect levels are depicted separately as follows:

(a) Defect level $E_1 = E_c - 0.14eV$

This defect level is induced by one-MeV proton irradiation in n-GaAs, and has been observed also in the electron-irradiated GaAs by other investigators [13-15]. The possible candidate for this defect level may be due to the arsenic vacancy related defect, as reported by Chang et al. [11] in the thermal annealed GaAs. The defect density of this level increases with increasing proton fluence for $\phi_o \geq 10^{13}$ cm^{-2}. The electron capture cross section for this level has a value around $5x10^{-13}$ cm^2 with strong electric field dependence. The electron emission rates also show some field dependence.

(b) Defect level $E_2 = E_c - 0.38eV$

This defect level was observed in both unirradiated and proton-irradiated n-GaAs samples. The electron capture cross section in this level is around $3x10^{-14}$ cm^2 with no field dependence observed. The level is a donor type defect center and may be due to gallium vacancy related defect associated with oxygen enhancement [11].

(c) Defect level E_3 = 0.46 to 0.60 eV below E_c

This defect level is introduced by proton-irradiation; its thermal activation energy varies from 0.46 to 0.60 below E_c as proton fluence increases from $5.8x10^{12}$ to $4.1x10^{15}$ cm^2. The reason for the change in ΔE is attributed to the fact that interaction between this defect level and E_4 appears to increase as the proton fluence is increased. The electron capture cross section for this level has a value around $6.5x10^{-15}$ cm^2 with strong field dependence. The possible candidate for this defect level may be associated with gallium and arsenic divacancy defect as reported by Chang et al. [11]. The density of this defect

level increases with increasing proton fluence for $\phi_o > 10^{13}$ cm^{-2}, as shown in the previous section.

(d) Defect level $E_4 = E_c - 0.65eV$

This defect level was observed in both unirradiated and one-MeV proton irradiated n-GaAs samples. Its physical origin may be associated with gallium vacancy defect [11]. This defect level has a thermal capture cross section of around 3.4×10^{-15} cm^2 with no field dependence and is believed to be a donor type center. The density of defect for this level remains nearly the same for both unirradiated and irradiated GaAs samples.

(e) Defect level $E_5 = E_c - 0.78eV$

This defect level has been identified as the oxygen donor level which was observed in both unirradiated and proton-irradiated GaAs samples. This is the deepest electron trap level observed in the present work. The level has the largest defect density among all the defect levels studied. The electron capture cross section is around 1.4×10^{-14} cm^2 with no field dependence observed. The density of this defect level shows little or no change with proton irradiation in GaAs.

The two sublevels $E_1^+ = E_c - 0.19eV$ and $E_2^- = E_c - 0.29eV$ have a much smaller trap density when compared with five other main electron traps. The electron capture cross section for E_1^+ level is found to be greater than that of E_1 level, while electron capture cross section for E_2^- is found to be smaller than that of E_2.

It is worth noting that the brief summary presented above for each defect level concerning defect properties in both proton irradiated and unirradiated n-GaAs Schottky diodes are only the preliminary findings of our study in which semiquantitative interpretation of the observed

experimental data is given. A more detailed analysis of the trap density and its spatial dependence as well as field dependence of thermal emission and capture rates will be included in the next technical report. It is anticipated that some modification or correction of the present conclusions may be necessary in the future report as more experimental data are taken during the course of this research project.

V. FUTURE PLANS

During the second phase of this research project (i.e., for the next twelve months) we plan to continue our present efforts to investigate defect properties and I-V characteristics in both electron- and proton-irradiated GaAs materials using Schottky-barrier or GaAℓAs-GaAs p-n junction structure and to correlate the measured defect parameters with the performance characteristics of the GaAℓAs-GaAs solar cells. For proton-irradiations, we plan to lower the implanted proton fluence to the range of 10^{8} to 10^{11} cm^{2} and proton-energy to a few hundred KeV. For electron irradiations, electron fluences in the range between 10^{12} to 10^{16} cm^{-2} and energy equal or less than 1 MeV will be used in our study.

In addition to the diagnostical tools described in this report we plan to expand our measurement techniques to include SEM beam-induced current measurement, surface photo-voltage (SPV), and photoconductivity (PC) methods to measure the minority carrier lifetimes and diffusion lengths in GaAs. From these proposed experiments we plan to study correlations among the measured defect parameters and their effects on the performance of GaAs solar cells and to identify the fundamental physical mechanisms that limit the conversion efficiency in the irradiated GaAℓAs-GaAs solar cells.

Details of our research plans to accomplish the research goals are described in our renewal proposal submitted to NASA earlier and will not be elaborated further here.

VI. TECHNICAL PAPERS, CONFERENCES, AND ACKNOWLEDGMENTS

A. Papers presented and submitted for publication:

1. S.S. Li, D.W. Schoenfeld, and K.L. Wang, "Detection of Radiation Induced Defects in One-MeV Proton Irradiated GaAs Solar Cell Material by Transient Capacitance Method," Proc. IEEE 13th Photovoltaics Specialists Conference; late newspaper, presented in Washington, D.C., June 5-8 (1978).

2. S.S. Li, D.W. Schoenfeld, W.A. Krull, F. Llevada and K.L. Wang, "Study of Defects Induced by One-MeV Proton Irradiation in n-GaAs Using Transient Capacitance Method," Proc. of the International Conference on Recombination in Semiconductors, Univ. of Southampton, U.K., August 29-Sept. 1 (1978).

3. S. S. Li, D. W. Schoenfeld and K. L. Wang, " Energy levels, Thermal emission rates and capture cross sections of electrons in One-MeV Proton Irradiated n-type GaAs", Appl. Phys. Lett., submitted, Sept.(1978)

4. S.S. Li, D.W. Schoenfeld, W.A. Krull, F. Llevada, and K.L. Wang, "I-V and Defect Characterization in Unirradiated and One-MeV Proton-Irradiated n-GaAs Schottky Diodes," Solid State Electronics, to be submitted (in preparation), September (1978).

B. Conferences attended:

Dr. S.S. Li, Principal Investigator, also attended the following conferences during this research period (Sept. 1, 1977 through August 31, 1977):

1. "International Conference on Solid State Devices," Aug. 29-31, Tokyo, Japan, presented a paper (1977).

2. "Semiconductor Interface Specialists Conference," Dec. 1-3, Miami (1977).

3. "American Physical Society Meeting," presented a paper Nov. 23-26, Miami (1977).

4. "International Conference on Si-SiO_2 Interface Physics," March 21-24, IBM Yorktown Heights (1978).

5. "IEEE 13th Photovoltaic Specialists Conference," June 5-8, presented a paper, Washington, D.C. (1978).

6. "International Conference on Recombination in Semiconductors," present a paper Aug. 29-Sept. 1, Southampton, U.K. (1978).

7. "14th International Conference on Physics of Semiconductors," September 4-8, Edinburg (1978).

C. Acknowledgment

The author would like to thank Mr. G.H. Walker and Dr. E. Conway for various technical assistance and discussions throughout this work. The support by NASA and the University of Florida EIES Special Project is also gratefully acknowledged.

VII. REFERENCES

1. R. Stirn, JPL Technical Report, Sept. (1977).
2. A.G. Milnes, NASA Semiannual Status Report (1975).
3. C.T. Sah, and J.W. Walker, Appl. Phys. Lett. 22, 38 (1973).
4. D.V. Lang, J. Appl. Phys. 45, 3023 (1974).
5. S.S. Li, Appl. Phys. Lett. 29, 126 (1976).
6. S.S. Li and H.F. Tseng, J. Appl. Phys. (1973).
7. S.M. Sze, Phys. of Semiconductor Devices, Wiley (1972).
8. C.T. Sah, L. Forbes, L. L. Rosier and A.F. Tasch, Jr., Solid State Electronics 13, 759 (1970).
9. H. Hovel, Solar Cells, Vol. 2, Academic Press (1975).
10. A.G. Milnes and D. Feucht, Deep Level Impurities in Semiconductors, Pergamon Press (1972).
11. L.L. Chang, L. Esuki, and R. Tsu, Appl. Phys. Lett. 19, 143 (1971)
12. C.I. Huang and S.S. Li, Solid State Electr. 16, 1481 (1973).
13. Aukerman, L.W., Graft, R.D., Phys. Rev. 127, 1576 (1962).
14. Aukerman, L.W., Davis, P.W., Graft, R.D., Shilliday, T.S., J. Appl. Phys. 34, 3490 (1963).
15. Stein, H.J., J. Appl. Phys. 40, 5300 (1969).
16. Brehm, G.E., Pearson, G.L., J. Appl. Phys. 43, 568 (1972).
17. Kalma, A.H., Berger, R.A., IEEE Trans. Nucl. Sci. NS-19, 209 (1972).
18. Berg, N.J., Lieberman, A.G., J. Appl. Phys. 46, 3475 (1975).
19. Brundnyi, V.N., Budnitskii, D.L. Krivov, M.A., Redko, V.B., Phys. Stat. Solidi A27, K95 (1975).
20. O'Brien, J.K., Corelli, J.C., J. Appl. Phys. 44, 1921 (1973).
21. Pruniax et al., 2nd International Conference on Ion Implantation in Semiconductors (Springer-Verlag, Berlin) 212 (1971).
22. Lang, D.V., Kimerling, L.C., Phys. Rev. Lett. 33, 489 (1974).
23. Kimerling, L.C., Petroff P., Leamy, H., J. Appl. Phys. Lett. 28, 297 (1976).

VIII. PERSONNEL

In addition to this principal investigator, three graduate students, D.W. Schoenfeld, W. Krull, and F. Llevada, who were supported in part by the NASA grant, have also made substantial contributions to this project. Schoenfeld is expected to complete his Ph.D. dissertation on proton irradiation study in GaAs by December, 1978, and Llevada will finish his M.S. thesis by August, 1978, also on the study of radiation damage in GaAs bulk material.